IN-NOVA
MSCA Doctoral Network

Active reduction of noise transmitted into and from enclosures through encapsulated structures.

Marie Skłodowska-Curie Actions

project no. 101073037

M5
Review and results validation on all device noise control systems
WP1 – Device noise reduction (in-out problem)

Lead beneficiary: SUT
Date and version: 30/07/2024 v1.0

Funded by the European Union

Preface

In this document we present the report related to milestone no. 5: Review and results validation on all device noise control systems – decision on integration strategy.

Devices in a wide range of applications, e.g., automotive, aerospace, and household appliances, must comply with strict conditions concerning the noise levels they emit. The focus of this report is on the reduction techniques of the in-out noise transmitted from the devices to the surroundings, addressing the passive noise control (PNC), active noise control (ANC), and noise-controlling casings. The report highlights advancements in these areas and discusses how recent developments integrate to enhance noise control. Additionally, simulation results are validated from the literature, and future research challenges are discussed.

Table of Contents

1 Introduction

Noise pollution is a critical global concern caused by the development of various industrial machinery and household appliances. Significant research has been accomplished to reduce the noise levels due to the major effects on both physiological and psychological health. In general, noise can be classified into two main categories based on its transmission from or into enclosures. (1) In-out noise, which refers to the noise transmitted from enclosures to the surroundings. This type of noise can be generated and/or radiated by various devices. (2) Out-in noise, which refers to the noise transmitted into enclosures through encapsulated structures. The enclosures in this category can be represented by vehicle and aircraft cabins. The main scope of this report concerns the in-out noise reduction techniques. The noise reduction techniques can be classified mainly into passive and active methods. The primary difference between these methods lies in the energy required for their operation.

Passive noise control (PNC) method provides solutions that do not require an external energy supply, typically achieving optimal noise reduction through modifications to the physical properties of the barriers separating the noise source from the surroundings [1]. This method incorporates thin plates, metamaterials, and sandwich panels as noise barriers. Thin plates demonstrate a complex frequency response to various excitation types, complicating the achievement of desired performance. The authors of [2] introduced a numerical method for analyzing the effect of additional masses on the vibration response of a thin vibrating plate. This method utilized the known frequencies and natural modes of vibration of the unloaded plate and the physical characteristics of the masses. In [3, 4], the authors analyzed the influence of additional concentrated masses analytically and numerically, respectively. In [5], the authors optimized the arrangement of the additional elements to shape the frequency response of the plates. The functionality of openings on the vibrating plate motivated the authors to introduce a novel method for designing the openings parameters for different systems' requirements [6]. In addition to thin plates, metamaterials are specially designed periodic structures that reduce noise and vibration within certain frequency ranges through Bragg scattering or Fano-type interference [7] and based on wave propagation in periodic structures [8]. The first report on using solid crystals arranged in a periodic structure as a noise barrier was introduced in [9]. The double-wall structures known as sandwich panels was of interest and under experimental testing with air-coupled core since 1946 [10]. The theory of sound transmission loss (STL) in sandwich structures was first introduced by the authors in 1950 [11]. This theory is based on understanding the impedance of a single panel within an air-coupled sandwich structure and has been validated through experimental studies.

Inserting an absorbent material in the airspace significantly improves both mechanical [12] and acoustical performance [13] when the walls are relatively light. However, it has little effect on heavy walls. The hybrid solution of combining sandwich panels with acoustic metamaterials is discussed in [14]. This involves the periodic placement of local resonators within the core [15]. Additionally, the core topology is optimized in various studies, such as those in [16, 17]. The passive control methods are effective in noise reduction for wide range of frequency, but their systems get more complicated for low frequencies [18]. Thus, active methods can be employed in such cases.

In 1936, the active noise control (ANC) technology was invented and patented [19]. It's based on the concept of canceling the noise by sound waves that have the same amplitude with an opposite phase. With the development of the digital signal processing hardware components, the adaptive ANC systems were first implemented effectively using least-mean-square (LMS) algorithm [20]. However, the physical path between the actuator and the error sensors can cause instability, which motivated researchers to develop the filtered-x least-mean-square (FxLMS) algorithm [20, 21, 22]. Hence, the reference signal to the controller is filtered through the model of the secondary path between the actuator and the error sensors, making the FxLMS the most popular ANC algorithm due to its stability and simple structure [23, 24, 25].

A multi-channel FxLMS with online secondary path modeling (SPM) using the auxiliary random noise technique and variable step sizes for each filter was shown to have a high convergence rate [26]. In [27], the authors addressed the increased residual error from auxiliary signal injection for online secondary path estimation to enhance the system performance. The interaction between decentralized controllers in ANC system was studied in [28]. The increased complexity of ANC systems with a larger number of actuators, controllers, and sensors elevated the need for distributed control algorithms. The authors analyzed the performance of decentralized architectures by deriving stability condition based on Gerschgorin circle theorem, which was proved to be sufficient for stabilizing small systems. Along with the development of wireless communication technology between various ANC system components, the authors proposed an ANC system over a network of distributed acoustic nodes [29, 30]. Recently, an augmented diffusion FxLMS algorithm with neighborhood-based adaptation and node-based combination was proposed in [31].

The placement of physical sensors around the devices is challenging. Therefore, technology such as virtual sensing (RV) can greatly enhance noise control algorithms. Additional filter (AF) and remote microphone (RM) methods are the two common virtual sensing methods used in ANC [32, 33]. The RM method utilizes monitoring microphones placed remotely from the virtual sensor locations and estimate the signals on the virtual position through the use of observation filter O which can be estimated as in [34]. The AF utilizes a model reference adaptive control technique [35]. In [33], the authors introduced ANC with relative path method (RP-VS) method that improved noise reduction when the noise frequency varies. With the rise of artificial intelligence, researchers have increasingly investigated its application in ANC. The selective fixed-filter active noise control (SFANC) model integrates pre-trained filters with Convolutional Neural Networks (CNN) for real-time filter selection [36], while a secondary path-decoupled ANC (SPD-ANC) uses deep neural networks to model secondary paths and stabilize the system [37]. Recently, the authors of [38] developed DNoiseNet algorithm to process the signals' data in time domain. Active Structural Acoustic Control (ASAC) is mostly performed using a passive noise barrier, vibration actuators, sensors and a control system, as in [39, 40]. ASAC can reduce noise transmission through a structure by controlling its vibrations. With careful implementation, ASAC not only reduce the noise in specific local areas but can achieve overall global reduction [41]. In 1994, the implementation of ASAC in device casings was first introduced and patented [42]. In general the noise casings can be categorized into rigid casings which have steel rigid frame and lightweight casings, as in Fig. 1.

(a) Rigid Casing Structure.

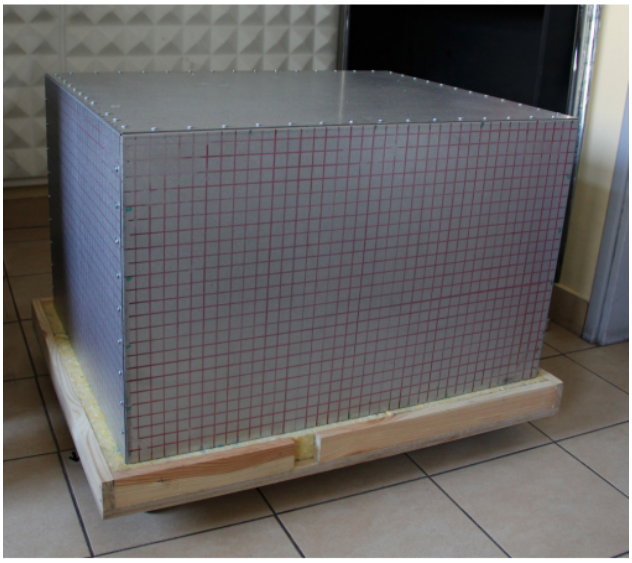

(b) Lightweight Casing Structure.

Figure 1: Photographs of rigid and lightweight device casings from the Laboratory at Silesian University of Technology.

The control for the whole device casing, named Noise-Controlling Casings, has been significantly developed and implemented with various control algorithms for the rigid casing [43, 44], and for a light-weight casing [45, 46]. Additionally, it can be applied to off-the-shelf devices as long as their casings' walls can be subjected to vibration forces [47]. In addition to PNC and ANC, semi-active barrier technology can also be applied to noise-controlling casings. This technology utilizes the inherent characteristics of the structure to meet the energy requirements for operation, typically needing only a small additional external energy supply [48]. Recently, the authors introduced semi-active actuators with a tunable mass moment of inertia, as detailed in [49, 50]. Survey articles usually cover passive or active noise reduction methods for both in-out and out-in noise. For ANC technologies, some articles report the history of the algorithms [18, 51, 52, 53], while others focus on the history of PNC [54, 55, 56]. In this article, the authors discuss various device noise reduction technologies, including PNC, ANC, and noise-controlling casings, thus paving the way for further advancements by integrating their recent developments. Additionally, the authors validate simulation work from the existing literature.

The report is organized as follows. Section 2 discusses passive noise control methodologies. The advancements in conventional ANC, including virtual sensing and deep learning techniques, are explored in Section 3. In Section 4, the noise-controlling casings are discussed with the active and semi-active methods. Finally, the authors summarize the conclusions in Section 5.

2 Passive noise control

The capability to shape the frequency response of thin plates is crucial for enhancing their effectiveness as noise barriers. The modification of the physical characteristics of the plates affect their acoustics response, this includes the mass and stiffness by adding additional elements. In early 70s, the authors of [57] analysed the dynamics of a plate stiffened by two sets of stiffeners analytically, while in 1977 the authors of [58] used FEM to analysis the vibration behavior of integrally machined rib-stiffened plates. In [59], the authors combined the effects of translational and rotational kinetic energies. The acoustical influence of additional elements has garnered wide interest among researchers, numerically [60], and using the radiation matrix for annular and rectangular plates [61]. The authors in [62] discussed different shapes and placements of ribs. The authors, in [63], modeled and optimized the arrangement of additional masses and ribs, in [5], to achieve precisely defined desired properties of the plate using an analytical approach and experimental validation, as shown in Fig.2 and Fig.3.

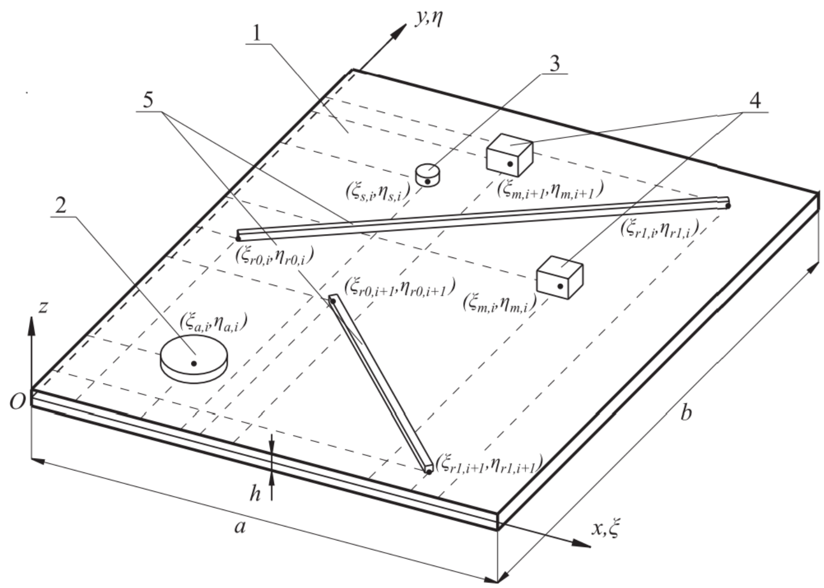

Figure 2: A thin rectangular plate(1) is modeled with various components: actuators(2), sensors(3), additional masses (4) and ribs(5) bonded to the surface. Reproduced from [63].

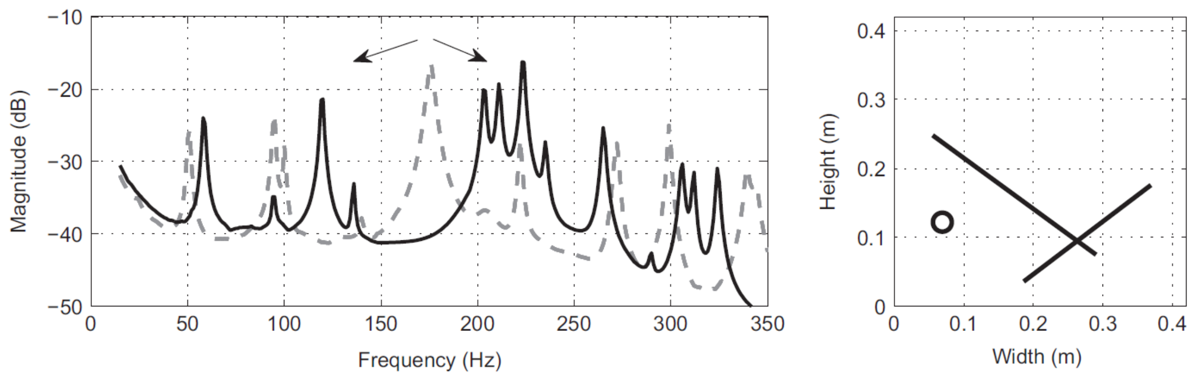

Figure 3: Experimentally measured frequency response of the plate (solid line – loaded plate; dashed line – unloaded plate) and visualization of additional elements mounted on the plate (circles – masses; lines – ribs). Reproduced from [5].

Incorporating openings in noise casings with vibrating plate structures is essential for engineering applications, facilitating heat dissipation, cable routing, personnel access, and weight reduction. Authors in [64] analytically studied the effect of having an opening on a vibrating plate that separates two adjacent rooms with only rectangular opening. In [65], the authors proposed a spectral-geometry method (SGM) for studying sound radiation from vibrating plates with arbitrary-shaped openings, but they overlooked the crucial structure-fluid coupling. Recently, the authors of [6] introduced and experimentally validated a novel analytical method for shaping the frequency response of vibrating plates with openings, demonstrating alternating frequency response through careful design of the opening shape and location. The simulation, in Fig. 4, is based on the proposed methodology and shows that the configuration with a continuous perimeter has its maximum resonating frequency at a lower amplitude than the other.

In the literature, the extraordinary acoustic properties of metamaterials have been extensively discussed. The broadband low-frequency absorption as in [66, 67, 68] and efficient sound insulation as in [69, 70]. In 2022, the authors of [16] introduced a topology design method of the space coiled acoustic metamaterial (SCAMM) unit along with the analytical calculation methods of sound pressure reflection and transmission coefficient of various SCAMM units.

The authors of [14] filled the space between two panels of a sandwich structure with porous material. They analyzed the performance of the structural-acoustic coupled system of a sandwich structure backed

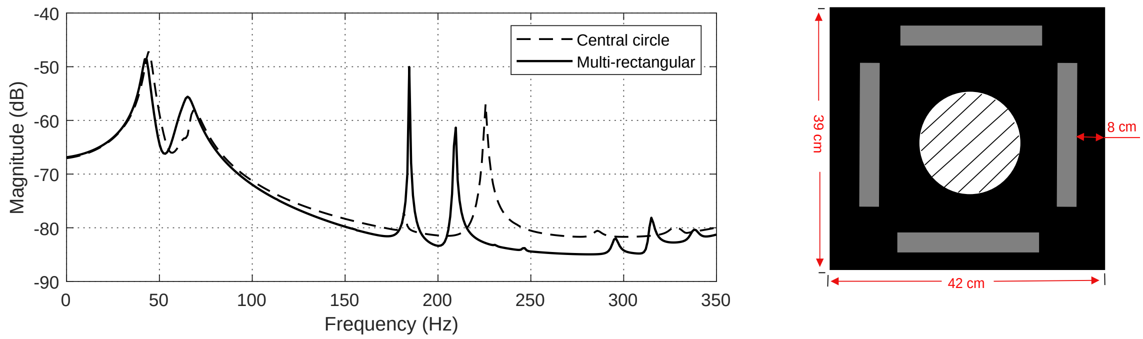

(a) Sound power response for the given opening designs.

(b) Central circular opening with a diameter of 0.1 m and multiple rectangular openings with a length of 0.2 m and a width of 0.01 m.

Figure 4: Comparison between two opening designs, each with a total area of 78.57 cm^2, showing the effect of multiple versus single openings on the sound power response. Based on the simulation settings of the analytical model as described in [6].

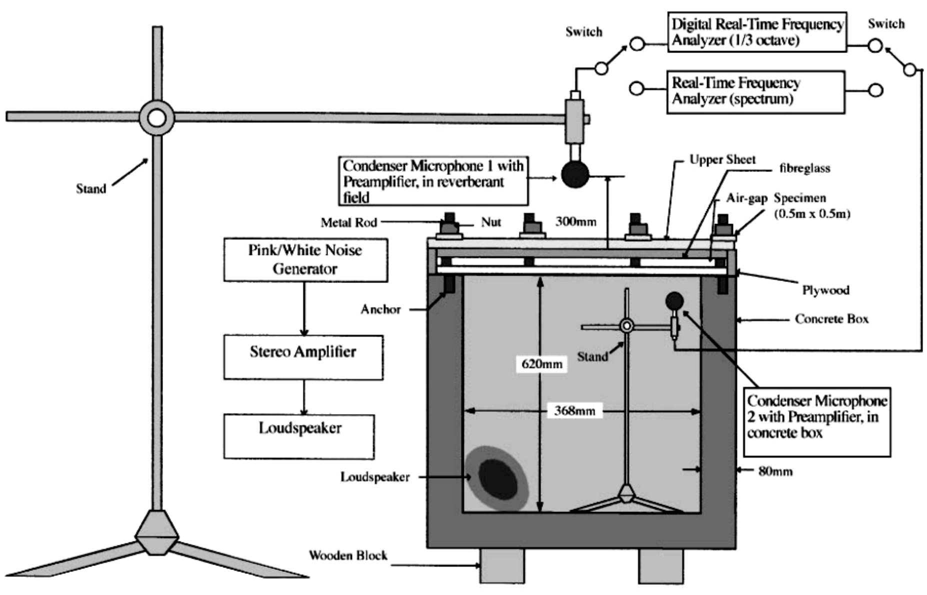

Figure 5: Description of an acoustic metamaterial (AMM) sandwich panel. Reproduced from [15].

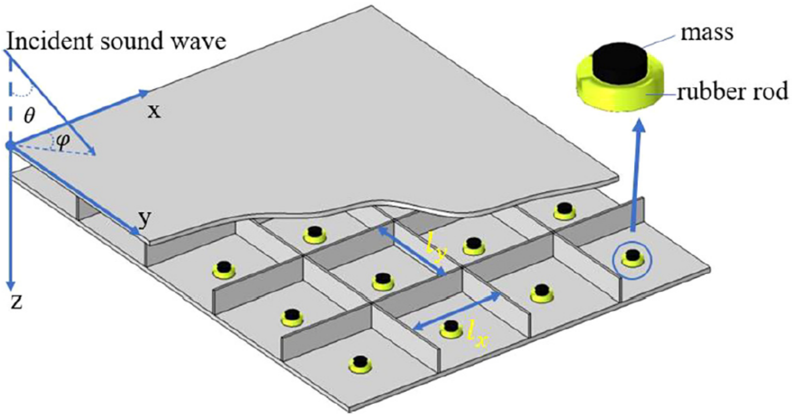

Figure 6: Schematic of the experimental acoustic measurement setup by the authors (not to scale). Reproduced from [14].

by a rectangular enclosure with rigid walls, as shown in Fig. 5. Their results indicated that a hybrid arrangement, with fiberglass bonded to the first panel and separated from the second panel by an air space, minimizes fundamental resonance without significantly impairing high-frequency performance. The authors in [15] proposed a novel strategy for designing an advanced acoustic metamaterial (AMM) sandwich structure, enhancing its STL through periodic placement of local resonators within the stiffened core as in Fig. 6. Their approach utilizes the space harmonic expansion method to analyze transmission properties, considers face sheet-core interactions, and validates findings through acoustic experiments and Finite Element Method (FEM) simulations.

Recently, the authors of [17] optimized the double panel configuration to achieve the maximum STL, as shown in Fig. 7. The design focuses on the core between the panels, with the panels themselves considered as passive domains. They achieved STL improvements of over 15–40 dB in targeted frequency ranges from 1000 Hz to 3000 Hz.

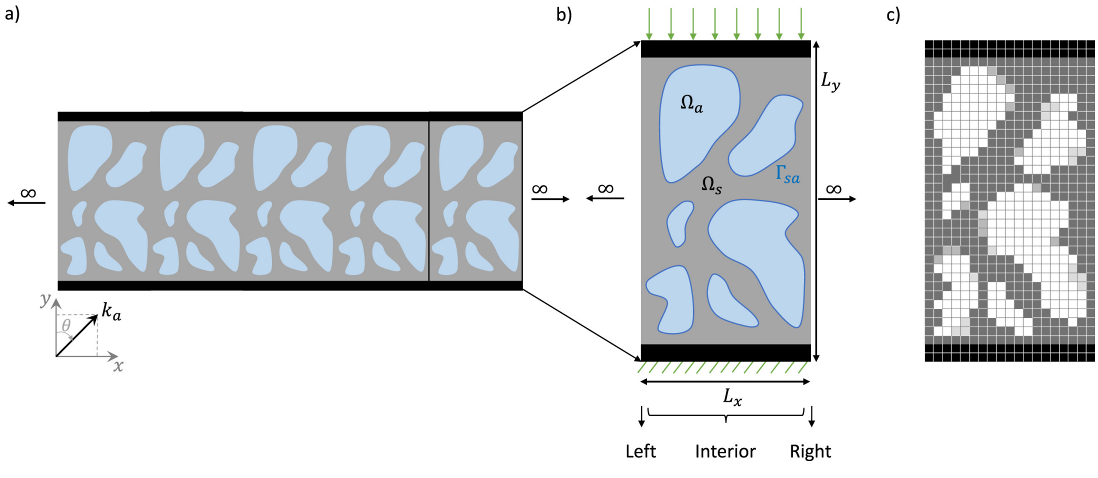

Figure 7: (a) Problem description. (b) Supercell considered in the authors' numerical model. The green indications symbolize the force and boundary condition used in the computation of the stiffness constraint. (c) Example of the structured FE discretization. Reproduced from [17].

3 Active noise control algorithms

3.1 Adaptive algorithms

3.1.1 Conventional algorithms

Adaptive algorithms such as LMS, Normalized LMS (NLMS), and FxLMS are fundamental in active noise and vibration control strategies [71]. The LMS algorithm updates filter weights iteratively using the steepest descent method, aiming to minimize the error between input signal $x(n)$ and error signal $e(n)$ as follows:

$$w(n+1) = w(n) + \mu x(n)e(n), \tag{1}$$

where $w(n)$ represents the filter coefficients at iteration n, μ is the step size controlling the rate of adaptation. The step size μ can be adjusted based on criteria such as the cross-correlation between $x(n)$ and $e(n)$, ensuring effective adaptation in varying noise environments as in [72]. NLMS can improve the LMS by normalizing the step size μ according to the power of $x(n)$ and μ can be calculated as follows:

$$\mu(n) = \frac{\alpha}{x(n)^T x(n) + \epsilon}, \tag{2}$$

where α is a constant and ϵ prevents division by zero, ensuring stability and improved convergence rates [73]. FxLMS extends these principles by using a filtered-reference approach. In FxLMS, the primary path $P(z)$ represents the acoustic transfer function between the reference microphone and the error sensor, capturing modifications in sound propagation. The secondary path $S(z)$ is the acoustic transfer function between actuators and the error microphone, while $W(z)$ denotes the digital adaptive filter. The error signal $E(z)$ can be identified as:

$$E(z) = [P(z) - S(z)W(z)]X(z), \tag{3}$$

where $X(z)$ is the reference signal in the frequency domain. Ideally, after convergence, $W(z)$ should equal $P(z)S^{-1}(z)$, ensuring the filter accurately models the primary path $P(z)$ and the inverse of $S(z)$. However, exact inverse modeling of $S(z)$ is often impractical. In [21], FxLMS method is introduced as an alternative approach. This method, illustrated in Fig. 8, dynamically adapts the filter coefficients $W(z)$ based on the difference between $P(z)$ and $S(z)W(z)$.

Different authors implemented and evaluated multi-channel versions of these algorithms in [74, 75, 76] and [77]. However, the multi-channel FxLMS-based algorithms, such as in [78, 79], are still preferred

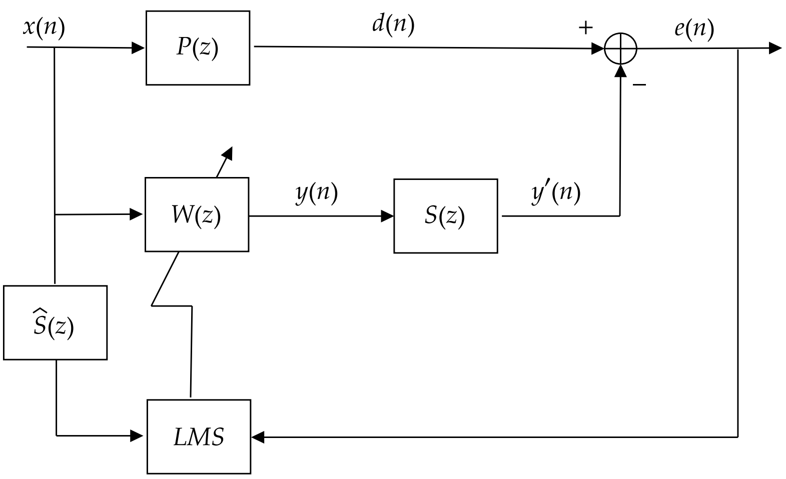

Figure 8: FxLMS for a broadband feedforward system, where $\hat{S}(z)$ represents the estimated secondary path.

in some applications due to their convenience and ease of implementation for some applications. These applications include air conditioning, washing machines, and compressor noise. Table 3.1 shows list of authors and their contributions for implementing multi-channel algorithms for their system. These authors adopted a multi-channel FxLMS-based algorithm for in-out noise propagation-based scenarios.

Table 3.1: Multi-channel FxLMS based algorithm for in-out noise reduction applications.

Year	Authors	Contribution	References
2004	E. Esmailzadeh, A.R. Ohadi and A. Alasty	Multi-channel adaptive feedforward control of an acoustic duct.	[80]
2007	B. Mazeaud and M.A. Galland	Multi-channel feedback algorithm for flow duct applications.	[81]
2011	N. Devineni, I. Panahi and P. Kasbekar	Multi-channel feedback ANC for HVAC systems.	[82]
2018	K. Mazur, S. Wrona and M. Pawelczyk	Design and Implementation of Multichannel Global ASAC for a device casing.	[41]
2020	C. Shi, Z. Jia, R. Xie and H. Li	Multi-channel feedfoward ASAC system using relative path based virtual sensing method.	[33]
2021	N. Botti, T. Botti, L. Liu, R. Corradi and F. Ripamonti	Active Structural-Acoustic Control on interior noise of a plate-cavity system using FxNLMS algorithm.	[83]

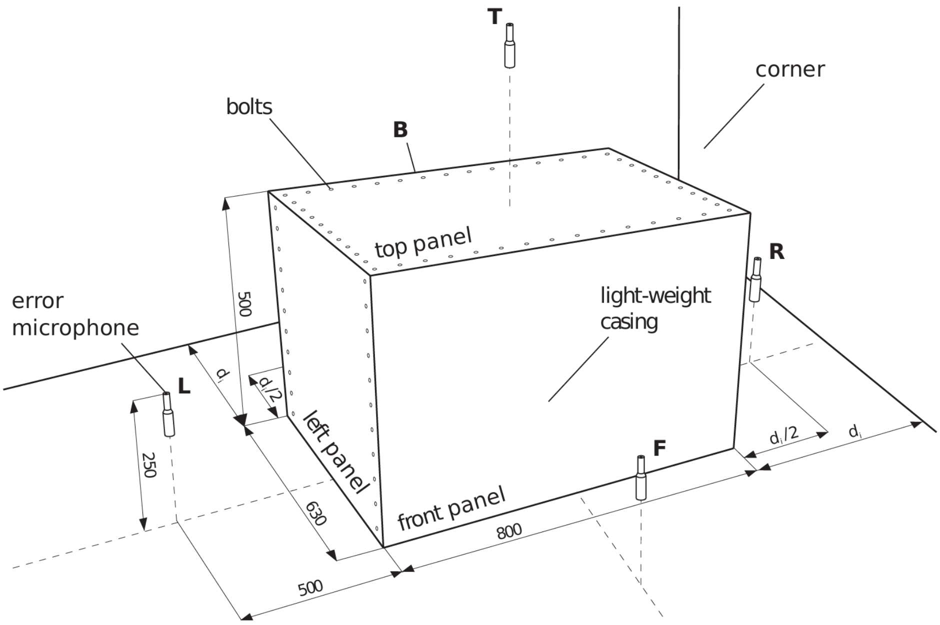

Figure 9: Microphones arrangement according to the experimental setup of a lightweight noise controlling casing. Reproduced from [84].

In these algorithms, and ANC in general, modeling the physical paths between the controllers and sensors is crucial as it determines the overall system performance. One of the most common modeling technique is using Finite Impulse Response (FIR) models.

Based on the experimental data, provided by the authors of [84], the authors are modeling the acoustic paths of the 5 microphones around a lightweight noise controlling casing, as in Fig. 9, with 128 coefficients FIR filters. From Fig. 10, it can be presumed that the variance of each microphone signal obtained from the simulation is validated with the experiment's responses.

The variations shown in the responses are mostly caused by minor errors of modelling obtained by system identification. As well, the decimation of the frequency response (5Hz frequency resolution) can slightly reduce the comparability of both responses. However, if the path changes over time, online modeling is needed [85, 86]. In the case of constant paths, offline modeling using identification techniques may be sufficient. However, in practical situations, modeling errors and other uncertainties should still be considered, according to the work in [23].

In [87], the authors demonstrated effective noise mitigation using LMS and FxLMS algorithms across a range of frequencies, achieving notable reductions at specific frequencies by employing optimal step sizes. Later, an error signal Differential term feedback Variable Step size FxLMS (DVSFxLMS) algorithm

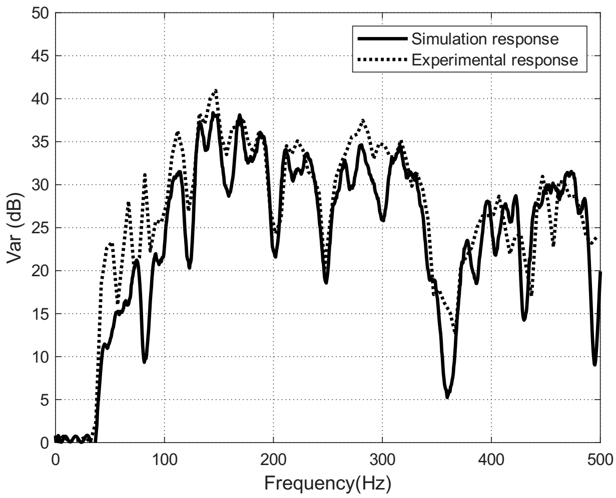

(a) Microphone F response.

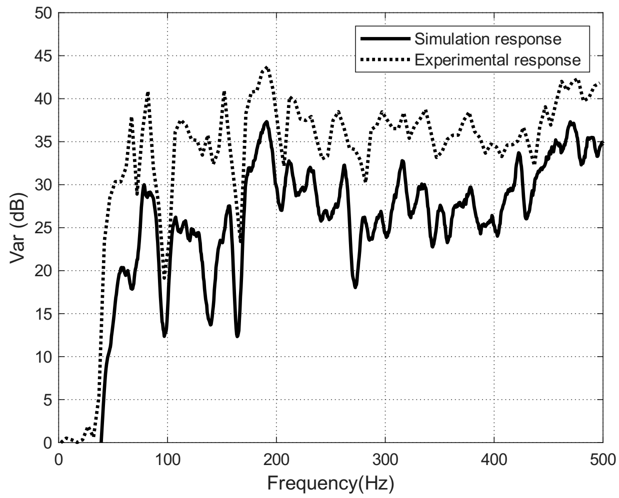

(b) Microphone R response.

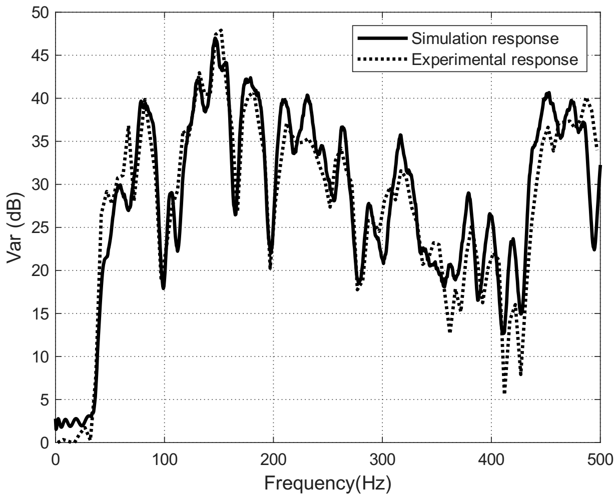

(c) Microphone B response.

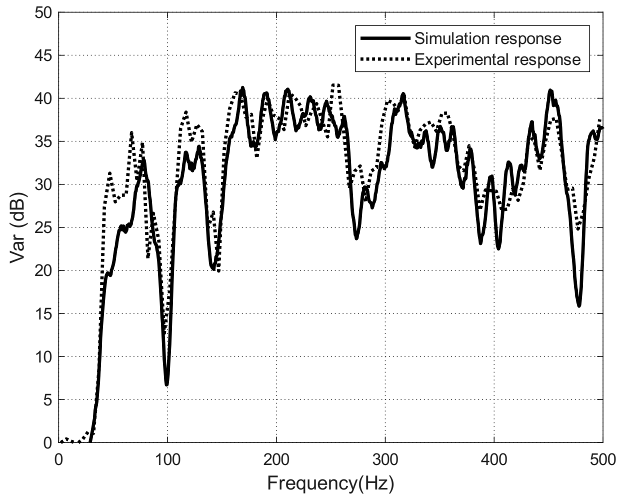

(d) Microphone L response.

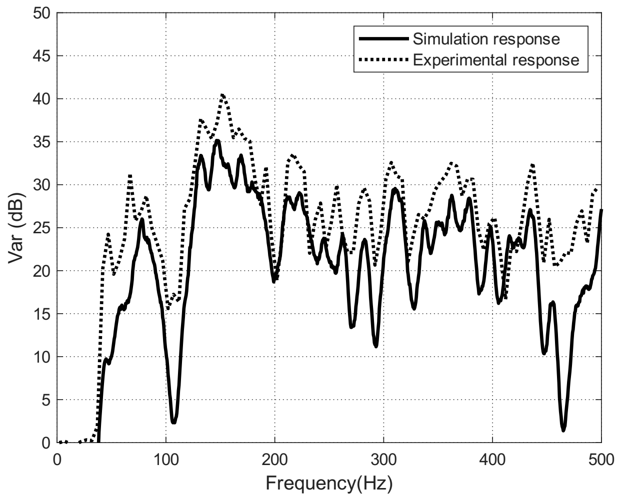

(e) Microphone T response.

Figure 10: Validation of FIR models for acoustic paths' responses with experimental measurements from [84], Var refers to the variance of the signals in dB.

established a nonlinear relationship between step size and error signal, achieving faster convergence and smaller steady-state errors in both simulations and experimental testing [88].

3.1.2 Distributed control algorithms

The authors, in [29, 30], derived and validated a collaborative condition based on the study of the eigenvalues of the acoustic paths along with a distributed Multiple Error FxLMS (DMEFxLMS) algorithm. This allows to create subsets of acoustically coupled nodes to reduce the computational requirements. Fig. 11 compares the decentralized, centralized, and distributed control architectures.

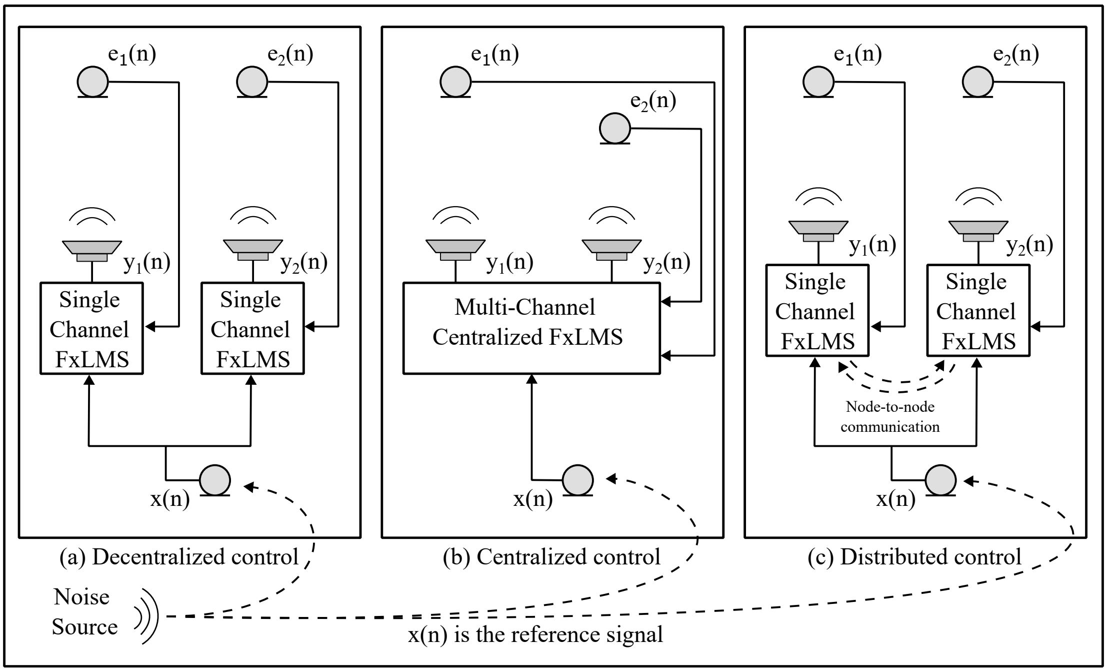

Figure 11: Schematic of decentralized, centralized and distributed architectures. Where the difference between (a) and (c) is the collaborative strategies between the decentralized controllers.

In [89], the authors introduced a collaborative approach based on diffusion algorithm which outperformed the non-collaborative strategies in systems that are highly coupled. Recently, the remote microphone (RM) technique was implemented in distributed networks [90].

Table 3.2: Contributions to distributed control ANC algorithms in the last decade.

Years	Authors	Contributions	References
2016	C. Antoñanzas, M. Ferrer, M. de Diego and A. Gonzalez	Introduced affine-projection-like algorithms for distributed ANC.	[91]
2017	C. Antoñanzas, M. Ferrer, M. de Diego and A. Gonzalez	Adjusted the distributed algorithm's cost function with node control effort weighting for power constraints.	[92]
2020	Y. J. Chu, C. M. Mak, Y. Zhao, S. C. Chan and M. Wu	Investigated the Diff-FxLMS algorithm for multi-channel ANC systems, proposing a systematic design procedure.	[93]
2021	Y. Dong, J. Chen and W. Zhang	Developed a wave-domain ANC system using multi-node networks each equipped with microphones, speakers, and a processor.	[94]
2023	J.Ji, D.Shi, Z.Luo, X.Shen and W.S. Gan	Developed a practical solution for distributed ANC algorithms overcoming communication restrictions.	[95]
2023	T.Li, S.Lian, S.Zhao, J.Lu and I.S. Burnett	Introduced Augmented diffusion FxLMS for distributed ANC systems.	[31]

The RM-DMEFxLMS algorithm achieved the same results as the centralized algorithm in networks with ring topology and incremental communication. The distributed control algorithms have more extensive work from researchers. Table. 3.2 highlights some research contributions to distributed ANC algorithms.

3.2 Virtual sensing based algorithms

In practice, positioning the error sensors at the optimal location for control can be challenging due to design constraints as the 10 dB zone of quiet tend to form locally around the error sensors at higher frequencies. To ensure global noise reduction performance, it would often desirable to place the error sensors beyond the design constraints. Virtual sensing techniques can help overcome these limitations by estimating the necessary error signals without the need for additional physical microphones.

3.2.1 Remote microphone technique

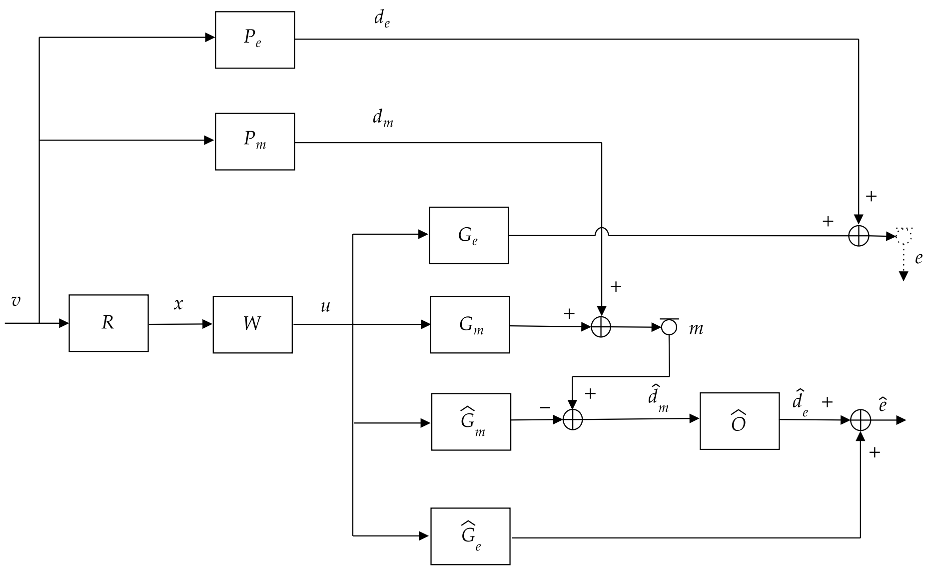

Figure 12: Block diagram of the remote microphone technique equipped in a feedforward control system. R is the modelling accuracy in obtaining the primary sources based on the existing reference signals; W is the control filter; P_e and P_m represents the acoustic paths from the primary loudspeakers to the virtual error sensors and physical monitoring sensors respectively; G_e and G_m represents the plant response from the secondary loudspeakers to the virtual error sensors and physical monitoring sensors respectively. The $\hat{}$ notation denotes the estimated plant obtained during the calibration stage.

The implementation of the RM in feedforward control architecture is illustrated in Fig. 12. For N_v primary sources, $\mathbf{v} = [v_1, v_2, \ldots, v_{N_v}]^{\mathrm{T}}$ is the vector of complex source strengths, producing a vector of N_e complex disturbance signals, $\mathbf{d}_e = [d_{e1}, d_{e2}, \ldots, d_{eN_e}]^{\mathrm{T}}$, at the virtual error microphones. Here, $\mathbf{e}$ is the vector of complex error signals at the virtual error microphones. For N_m monitoring microphone signals, $\mathbf{m} = [m_1, m_2, \ldots, m_{N_m}]^{\mathrm{T}}$ and $\mathbf{d}_m = [d_{m1}, d_{m2}, \ldots, d_{mN_m}]^{\mathrm{T}}$ is the vector of disturbance signals measured at the monitoring microphones. The frequency dependence of these signals and responses is suppressed for brevity.

Although the RM is used to solve the difficulty of placing physical microphones in some locations, it is also subjected to various physical limitations. For the case of a perfectly diffuse primary sound field, the remote microphone technique is not able to provide good estimation when either the frequency is increased or the distance between the monitoring microphone and the virtual error microphone is too large [34]. This is illustrated in Fig. 13a, which shows that the region where the estimation error of -10 dB depicted by the gray region increases significantly when multiple monitoring microphones were used as compared to the single monitoring microphone case shown in Fig. 13b.

Since the observation filter is calibrated based of the spatial properties in the primary sound field, the estimation performance will degrade subject to changes in the primary field. Such changes could be either due to the changing primary source position [33, 96] or by moving objects that cause additional scattering inside the primary field [97]. The authors of [33] introduced the relative path virtual sensing technique (RP-VS) by additionally obtaining the observation filter when only the secondary sound field is present.

In the context of a vehicle cabin local control application, where the main noise source varies based on road conditions, the authors of [98] suggested a min-max classification approach. When the primary sound field changes due to the introduction of additional noise sources within the casing, it is found that the estimation accuracy from the observation filter can degrade significantly [96].

Funded by the European Union

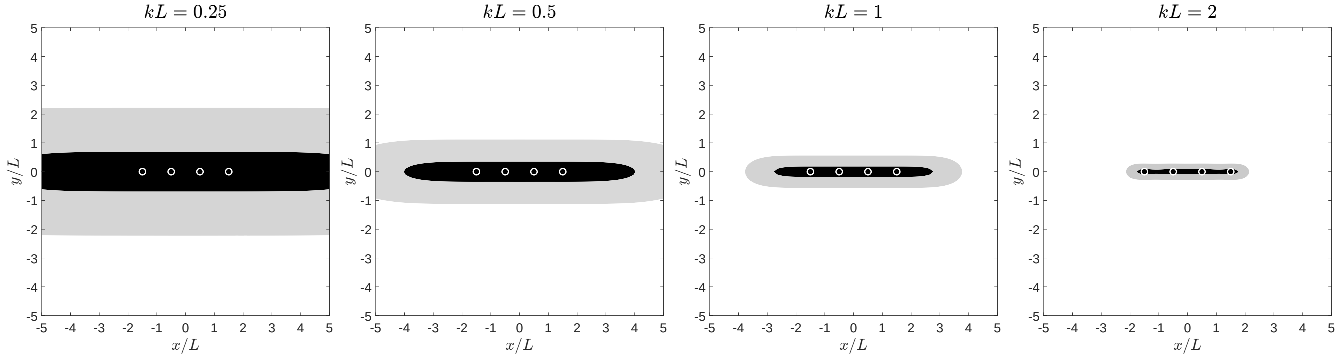

(a)

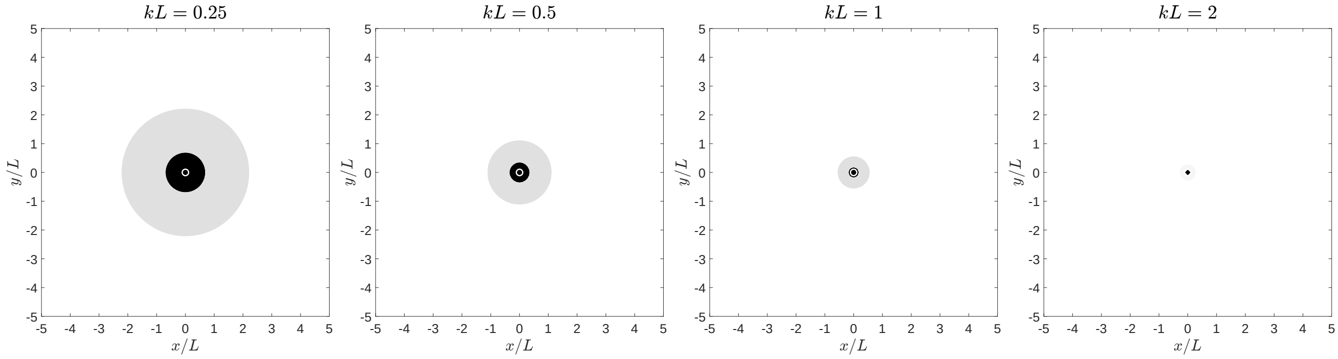

(b)

Figure 13: The -20 dB error zone (black region) in the 2D spatial grid indicates where an estimation error of -20 dB or less is achieved. The -10 dB error zone (grey region) indicates where an estimation error between -20 and -10 dB is achieved when (a) 4 monitoring microphones and (b) a single monitoring microphone were used. The monitoring microphone were depicted by the white circles, k is the wavenumber, and L is the separation distance between the linear monitoring microphones. The simulation settings and parameters under diffused field condition is based in the work in [34].

3.2.2 Additional filter

The goal of the additional filter is to capture the state of the physical monitoring microphone where the signal at the virtual error sensor is minimized. During the tuning stage, the initial control filter $\hat{W}_{AF}$ is obtained by minimizing the error signals and an additional filter $\hat{H}$ which models the response from the reference signals to the monitoring signals, as illustrated in Fig. 14. The additional filter showed superior robustness against small perturbations of the acoustical paths between the monitoring microphone and the error microphone [99]. However, in practice, the plant response can be perturbed due to changes in circumstances, hence the controller performance becomes extremely sensitive to the reference signal characteristics.

The authors of [100] introduced a set of pre-trained additional filters, each accommodating the reference signal for a different range of frequencies, as such that the summation of these additional filters will match the frequency spectra of the reference signal. Alternatively, deep learning techniques can be deployed [101] to quickly distinguish different noise classes and primary sources, which help select the optimal additional filter more accurately. Since the additional filter is based on model reference adaptive control technique, it is free from the causality constraint that the remote microphone technique is subject to [102].

3.3 Deep learning-based algorithms

In [103], the authors employed a feedforward controller utilizing deep learning algorithms to estimate the primary noise, as in Fig. 15. In [104, 105], the authors the complex mapping method which involves computing the spectrogram of radiated sound and dividing it into real and imaginary components and highlighted its effectiveness in speech enhancement by training Convolutional Recurrent Network (CRN).

Central to achieving a suitable model for the control is the definition of the loss function, as represented

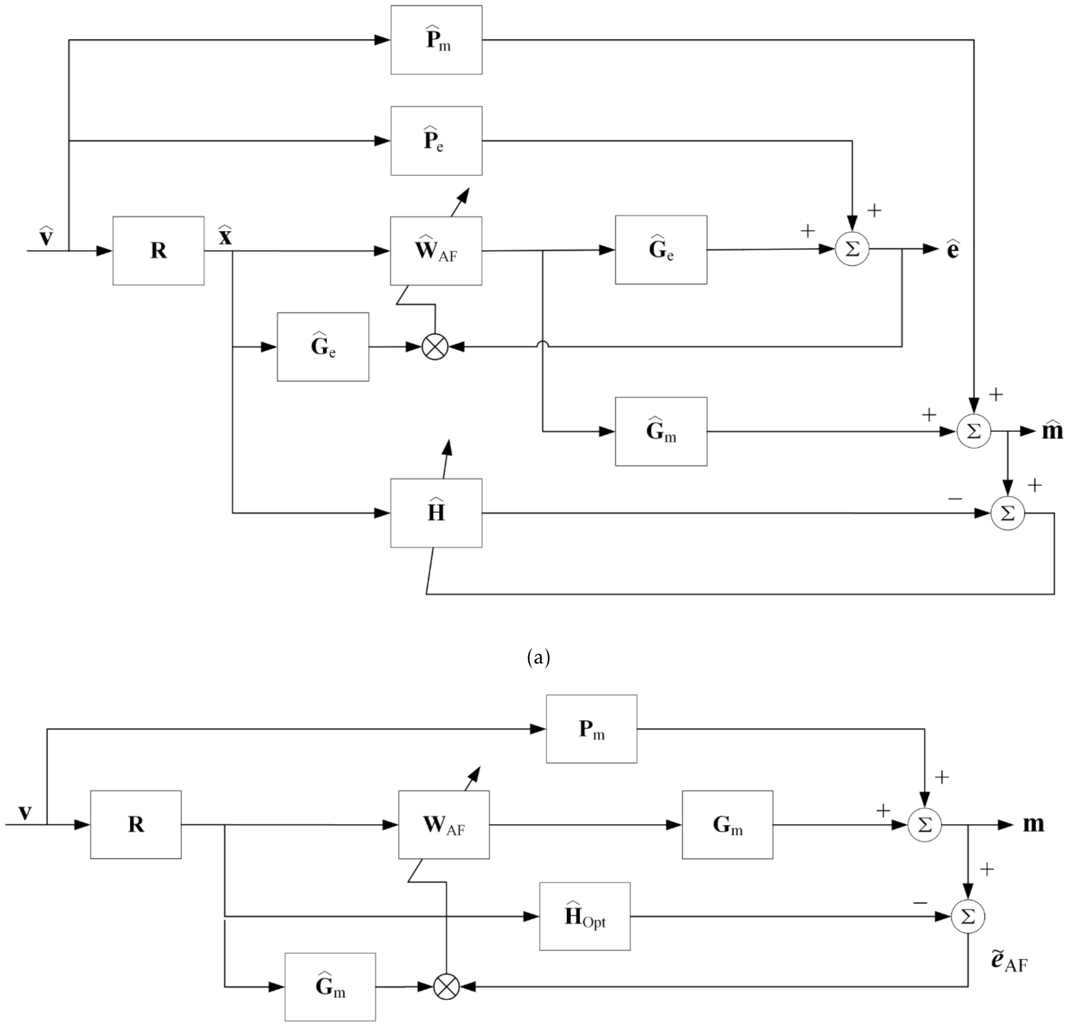

(a)

(b)

Figure 14: The block diagram of the additional filter method for (a) the tuning stage and (b) the control stage, where $\hat{H}_{opt}$ is the optimal additional filter and $\tilde{e}_{AF}$ represents the difference between the signals measured at the monitoring microphones and the estimated signals when the error is minimized. Reproduced from [99].

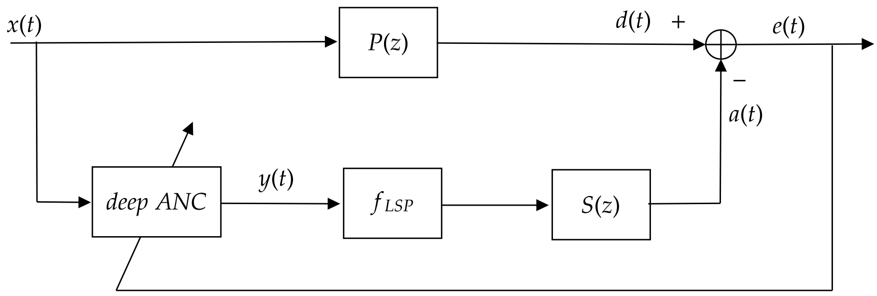

Figure 15: Diagram of the deep ANC approach, where the signals are in the time domain and f_{LSP} simulates loudspeaker-related nonlinearities. Reproduced from [103].

by Eq. 4:

$$e(t) = p(t) * x(t) - s(t) * f_{LSP}\{a(t)\}, \tag{4}$$

where $p(t)$ represents the transfer function of the primary path in time domain, $s(t)$ stands for the transfer function of the secondary path, and $a(t)$ denotes the anti-noise generated by the controller. This loss function is crucial during model training as it integrates all facets of the control environment. Table. 3.3

compares the effectiveness of the the deep ANC model trained with noise (CRN-n) against traditional algorithms like FxLMS and the tangential hyperbolic function based FxLMS (THF-FxLMS), showing good performance even at lower frequencies.

Table 3.3: Average normalized mean squared error (NMSE) (in dB) for deep ANC and traditional algorithms across different types of noise and nonlinear distortions. Noise types include Engine, Factory, Babble, and Steady-State Noise (SSN), with varying levels of η^2 (nonlinear distortion factor) represented as ∞, 0,5, and 0,1 [103].

Noise Type	Engine			Factory			Babble			SSN		
η^2	∞	0.5	0.1	∞	0.5	0.1	∞	0.5	0.1	∞	0.5	0.1
FxLMS	-6.78	-5.26	-4.54	-5.88	-4.73	-1.67	-6.04	-4.32	-3.37	-5.95	-4.38	-3.46
THF-FxLMS	-	-6.70	-6.55	-	-5.86	-5.75	-	-6.02	-5.97	-	-5.98	-5.94
CRN-n	-11.07	-10.98	-10.60	-9.58	-9.50	-9.17	-9.49	-9.45	-9.27	-9.90	-9.83	-9.56

Although the algorithm effectively manages noise without perceptible delay, the constraints on the sampling frequency of the input data are challenging for this approach. Hence, the development of the DNoiseNet algorithm, which has the ability to directly process data in the time domain, can address these challenges [38]. Fig. 16 shows two control algorithms that were developed and validated based on the DNoiseNet.

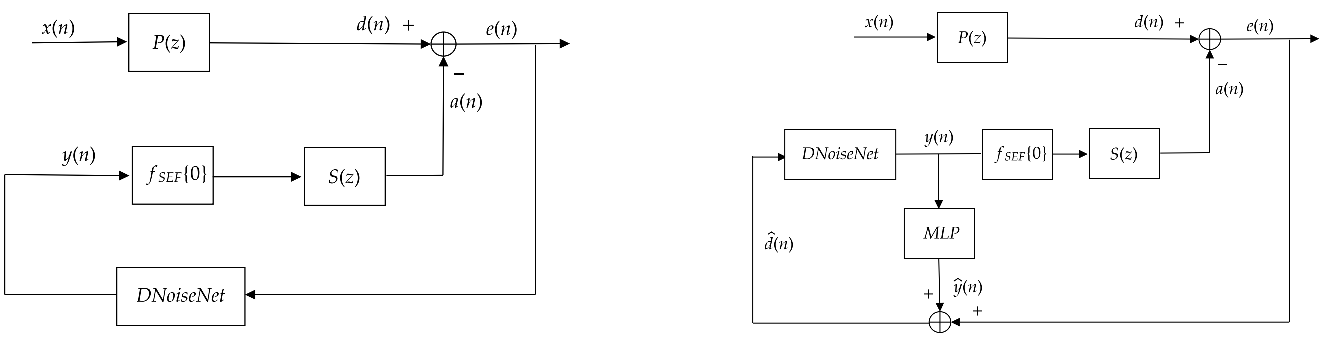

(a) DNoiseNet feedback control

(b) DNoiseNet feedback control with MLP

Figure 16: Block diagrams of the DNoiseNet ANC systems where f_{SEF} is the function of the loudspeaker [38].

The DNoiseNet feedback control, as in Fig. 16a, uses the deep learning algorithm directly as a controller, where Atrous Scaled Convolution (ASC) modules are used for capturing multidimensional features and nonlinearities present in input signals through the use of nonlinear activation functions as in [106]. The second strategy, as in Fig. 16b, is designed to provide the controller with information about the reference signal $\hat{d}(n)$. Adding a secondary path estimator based on multilayer perceptron (MLP) neural network reproduces the output signal of DNoiseNet, $y(n)$, with effect of the secondary path. Once reproduced, $\hat{y}(n)$ is added to the error to obtain a good estimation of the primary noise, $\hat{d}(n)$.

DNoiseNet algorithms were tested on various noise datasets: Leopard (military vehicle noise), Volvo (vehicle interior noise), Construction (cutting and welding noise), and the rest listed in Table 3.4 are various flight noises. For detailed information about the noise data, refer to [38].

Both algorithms demonstrated good noise attenuation, but DNoiseNet-MLP achieved better results across different types of noise, as shown in Table 3.4. Both algorithms achieved better results compared to normalized FxLMS (NFxLMS), artificial neural networks (ANN), long short-term memory (LSTM), and CNN-based ANC methods in terms of noise reduction. Unlike NFxLMS, they handle varying noise environments efficiently, and DNoiseNet-MLP provides higher robustness than ANN. Recently, hybrid algorithms that combine traditional ANC methods with advanced deep learning techniques have strongly gained researchers' attention. The deep-online learning method integrates pre-trained deep learning models with online learning to improve the adaptability and performance of ANC systems [107]. The authors, in [108], designed an attentive recurrent network (ARN) for low-latency ANC, which combines deep learning with strategies like delay-compensated training and a revised overlap-add method, to achieve minimal latency without compromising performance.

Another innovative approach highlights Physics-Informed Neural Networks (PINNs) for soundfield in-

Table 3.4: The dB levels of noise reduction achieved by various methods [38]. In bold, is the best noise reduction for each case.

Data	**DNoiseNet-MLP**	**DNoiseNet**	**LSTM**	**ANN**	**CNN**	**NFxLMS**
Leopard	**21.61**	14.59	20.44	21.57	17.14	-0.06
Volvo	**19.50**	16.22	16.08	17.60	16.22	1.45
Construction	9.42	8.62	8.61	**9.86**	9.14	0.40
Flight1	**21.38**	10.29	21.21	11.88	17.53	0.04
Flight2	**30.58**	13.99	27.39	20.57	24.28	4.20
Aero1	**30.03**	13.16	25.43	25.46	22.00	1.91
Aero2	**29.96**	16.97	27.03	27.19	24.11	1.25
Aero3	**26.44**	15.78	24.68	25.75	20.54	1.77
Aero4	20.81	14.11	**21.40**	16.26	17.16	1.94
Average	**23.30**	13.75	21.36	19.57	18.68	1.43

terpolation, that allows the placement of monitoring microphones outside the region of interest (ROI) [109]. Thus, there is a high potential for hybrid and physics-informed models to overcome the limitations of traditional ANC algorithms.

4 Noise controlling casings

4.1 Semi-active control

The recent work in [50] introduced semi-active actuators with a tunable mass moment of inertia, which can adjust the panel's response.

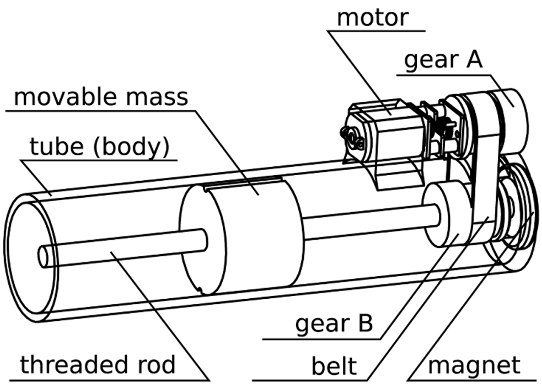

(a) Tuneable mass moment of inertia semi-active element. Reproduced from [49].

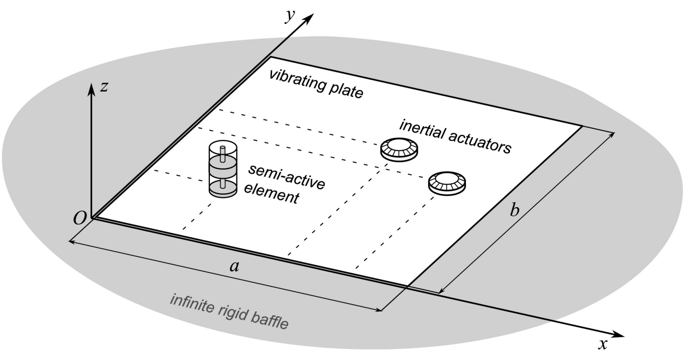

(b) Schematic of the semi-active element, as in (a), positioned on a plate in infinite baffle. Reproduced from [50].

Figure 17: Tuneable mass moment of inertia implementation in semi-active systems.

This adjustment improves noise transmission loss and optimizes acoustic radiation. This adjustment happens by controlling the distance z_s between the mass and the plate. The mass features a central threaded hole, as shown in Fig. 17a, which allows it to be mounted onto a threaded rod. This rod can be rotated by a micro motor to adjust z_s. In [50], the authors presented a novel hybrid active/semi-active noise control system for noise barriers, combining high performance with reduced energy consumption. The semi-active element adapts to time-varying narrowband noise by altering the mechanical response of the plate, enhancing transmission loss. They optimized the the semi-active element position along with different number of structure actuators N_a, as shown in Fig. 18. The semi-active element provides a better improvement in all cases. However, they considered only the noise to be periodical, which eliminates the potential issue associated with the variation and uncertainty in reference signals.

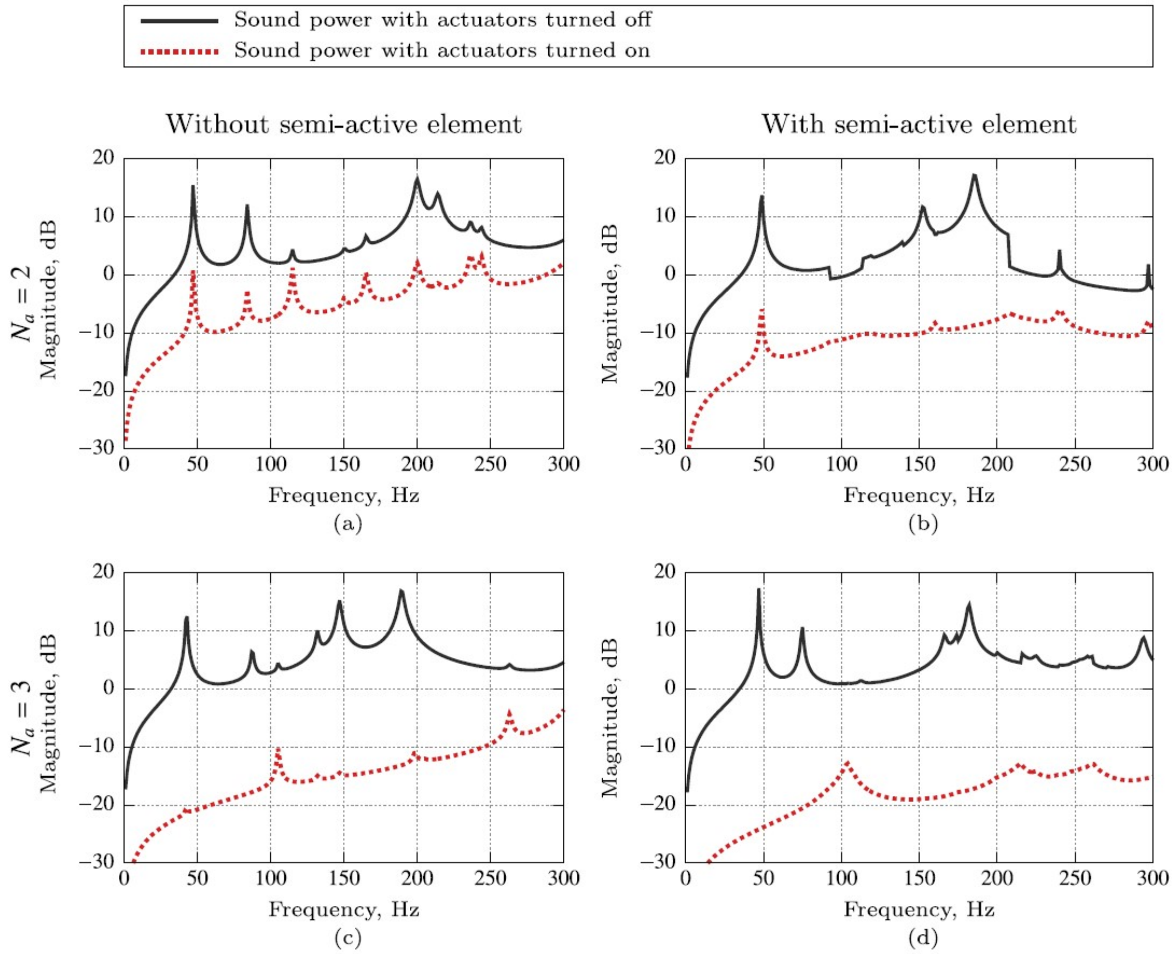

Figure 18: Acoustic responses of the panel when using multiple actuators, both with and without the semi-active element. (a) $N_a = 2$, without the semi-active element. (b) $N_a = 2$, with the semi-active element. (c) N_a= 3, without the semi-active element. (d) $N_a = 3$, with the semi-active element. Reproduced from [50].

4.2 Active control

Among the three method of noise reduction utilized in noise-controlling casings, active device casings are demanding the highest energy to operate. ANC and ASAC utilize actuators, such as inertial actuators, to emit anti-noise waves. When these waves have the same amplitude and and are opposite in phase, they reduce the sound pressure level through wave superposition [110]. Active control is particularly effective for low-frequency noises, making it an essential complementary method to passive control.

Both systems commonly use the FxLMS algorithm as in [78, 45], primarily due to ease of implementation and reliability [111]. With the increased number of error sensors and actuators, the Multiple Error FxLMS (MEFxLMS) algorithm becomes computationally intensive. One way to address this issue is to utilize only one error signal at a time, along with a designated interval for switching between error sensors. The authors, in [41], declared this approach as Switched-Error FxLMS (SEFxLMS). The algorithm was tested on the active casing noise control model, exhibiting the same steady-state noise reduction as MEFxLMS algorithm. However, the slow adaptation rate of the SEFxLMS leads to a significant reduction in convergence rate as a trade-off to the reduced computational complexity. The Switched Multiple Error FxLMS (SMEFxLMS) is an extension to the SEFxLMS algorithm [112], it has a convergence rate and computational load between the performances of the SEFxLMS and the MEFxLMS. Fig. 19 compares the performance of the MEFxLMS with SEFxLMS and SMEFxLMS reductions for simulations performed for a lightweight casing at a 150 Hz tone disturbance.

The switching algorithms contains power fluctuations due to the error switching effect. The algorithm that uses two error switching Q_{2B} performs better than Q_{2A} with only one switching error. In general, the SMEFxLMS performs a slower adaptation than the MEFxLMS, but it has a significantly reduced computational load. Thus, it can be used in applications where the changes in the noise signal are slower than

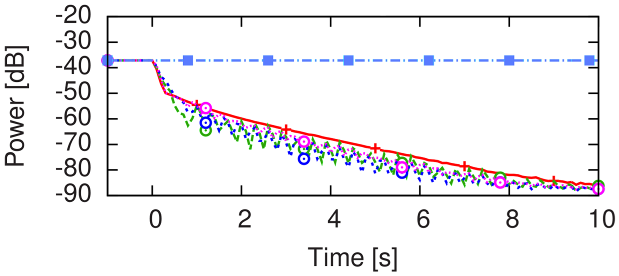

(a) Reductions obtained at Front microphone.

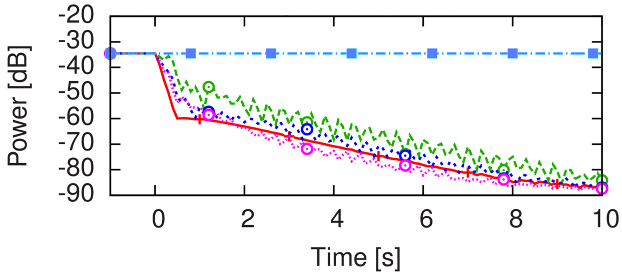

(b) Reductions obtained at Right microphone.

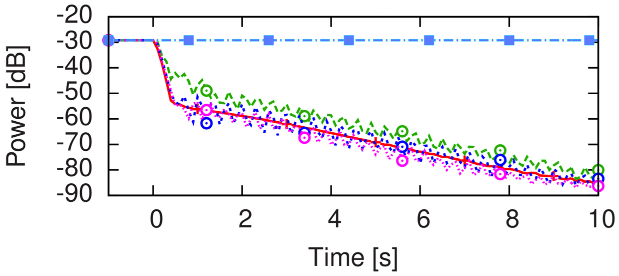

(c) Reductions obtained at Back microphone.

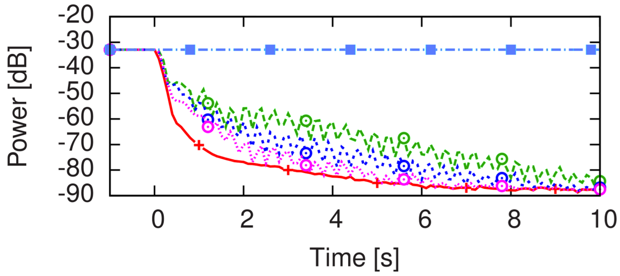

(d) Reductions obtained at Left microphone.

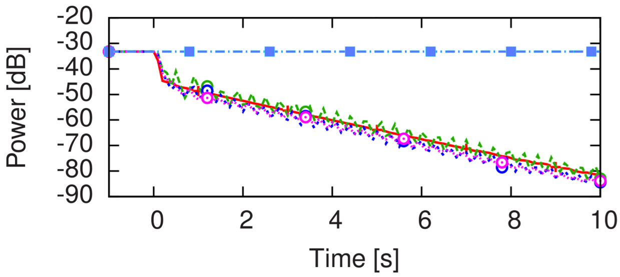

(e) Reductions obtained at Top microphone.

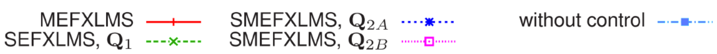

Figure 19: Adapted from [112], reductions obtained at each microphone using SMEFxLMS algorithm at 150 Hz single tone disturbance (using lightweight casing) and normalized step size $\mu_n = 0.005$. Where Q1 is typically the same as the SEFxLMS algorithm. Q2A allows adaptation for two sensors with one error switching. Q2B allows adaptation for two sensors and switching with two error signals. For the arrangement of the microphones and the testing setup, refer to [45].

the switching interval and adaptation speed. Alternative solutions are employing partial update (PU) algorithms. The PU algorithms are demanding for systems with high computational power requirements as they can further reduce the computational complexity [113, 114, 115]. The algorithm skips the update of certain control filter coefficients based on specific criteria. By skipping updates of some coefficients, the PU algorithm can further increase the convergence rate in some cases depending on the input signal. In [116], the authors updated the two partial-update augmented complex-valued LMS (PU-ACLMS) algorithms using less number of input samples to update by predicting the stochastic behaviour of the algorithm. The leaky versions of the PU LMS were introduced and applied to the ASAC application [117, 118]. Table 4.1 shows the original algorithms that was associated with partial updates for active device casing application [117].

Fig. 20 shows a sample spectrograms of a signal recorded at the fifth error microphone of a washing machine with and without active control. The system used thirteen actuators and eight microphones positioned in a quarter-sphere arrangement (For more information about the microphone arrangements and the physical setup of the washing machine in the testing room, refer to [117, 129]). The system used PU selective leaky NLMS (LNLMS) with M = 8. Where M is the amount of partially updated coefficients of a filter, this means 8 out of 256 coefficients are updated for each control filter. From the spectrograms, it is clear that the PU algorithm can reduce most of the harmonics induced by the washing machine, with an attenuation variance of up to 30 dB, which is considered a broadband attenuation of the signal.

Table 4.1: Algorithms tested, in [117], with PU.

Year	Authors	Algorithm	References
1971	B. Widrow and T. Hoff	LMS	[119, 73]
1971	B. Widrow and T. Hoff	NLMS	[119, 120]
1995	S.C. Douglas	OTU (One Tap Update) LMS	[121, 122]
1995	S.C. Douglas	max NLMS	[121]
1998	T. Aboulnasr, K. Mayyas and T. Eldos	M-max NLMS	[123, 124]
1997	T. Aboulnasr and K. Mayyas	Leaky LMS	[125]
1997	T. Aboulnasr and K. Mayyas	Selective LMS	[126]
1997	S.C. Douglas	Sequential & Periodic LMS	[127, 128, 114]
2005	M. Godavarti and A.O. Hero	PU LMS algorithms	[114]

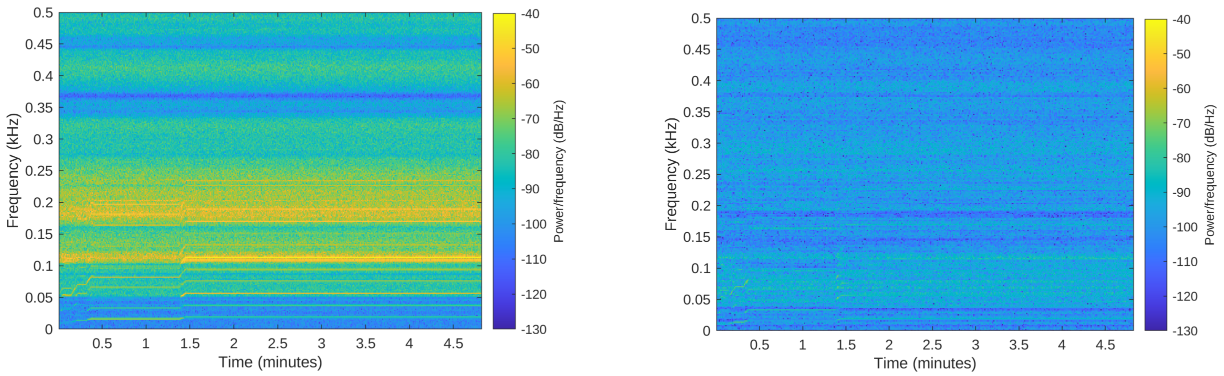

(a) Spectrogram of the disturbance signal without control.

(b) Spectrogram of the attenuated noise.

Figure 20: Spectrograms recorded at the fifth error microphone of a washing machine using the Selective LNLMS algorithm (from 0 to 500 Hz). Reproduced from [117].

5 Conclusion

In this report, the authors reviewed the recent advancements of the device noise control. With emphasize on the active noise control (ANC) algorithms, the passive noise control (PNC) and noise-controlling casings.

5.1 Summary

This work highlighted the advantages and drawbacks of each technique, providing insights for better decisions on integrating these technologies to achieve better noise reduction. Careful design of passive noise barriers can enhance noise reduction using metamaterials, sandwich panels, and vibrating plates without the need for energy sources, although these are mostly effective in high-frequency ranges. ANC can complement PNC and effectively reduce noise levels, but in device noise control, there is a risk of creating only local zones of quiet. Finally, noise-controlling casings require setting the devices within structured enclosures, however, providing the ability for global noise reduction in the whole room or environment.

5.2 Future work

The integration of different techniques can indeed enhance noise reduction. Since noise-controlling casings provide global noise reduction, incorporating metamaterial walls along with active structural acoustic control (ASAC) can be highly beneficial for reducing noise across a wide range of frequencies. When openings in the casing walls are necessary, optimizing the design of these openings should be the first step in creating effective noise-controlling casings.

To counteract the difficulty of placing physical sensors around the casings, especially in applications where the space around the devices cannot be customized, virtual sensing (VS) has shown high potential to replace these sensors with remote sensing (RM) or additional filtering (AF). Additionally, deep learning-based online path identification is a promising enhancement for noise-controlling casing techniques, making the systems more robust to variations in working environments. In-depth research and experiments are needed to test the reliability of these potential solutions.

References

[1] Z. Liu, H. Lee, C. Lu, Passive and active interior noise control of box structures using the structural intensity method, Applied Acoustics 67 (2) (2006) 112–134. https://doi.org/10.1016/j.apacoust.2005.04.010.

[2] W. Stokey, C. Zorowski, Normal vibrations of a uniform plate carrying any number of finite masses, Journal of Applied Mechanics (1959). https://doi.org/10.1115/1.4011984.

[3] C. G. Boay, Frequency analysis of rectangular isotropic plates carrying a concentrated mass, Computers & structures 56 (1) (1995) 39–48. https://doi.org/10.1016/0045-7949(94)00533-9.

[4] S. De Rosa, F. Franco, D. Capasso, S. Costagliola, The effect of concentrated masses on the response of a plate under a turbulent boundary layer excitation, Mechanical systems and signal processing 25 (4) (2011) 1192–1203. https://doi.org/10.1016/j.ymssp.2010.11.011.

[5] S. Wrona, M. Pawelczyk, Shaping frequency response of a vibrating plate for passive and active control applications by simultaneous optimization of arrangement of additional masses and ribs. part ii: Optimization, Mechanical Systems and Signal Processing 70-71 (2016) 699–713. https://doi.org/10.1016/j.ymssp.2015.08.017.

[6] K. S. A. Maamoun, S. Wrona, M. Pawelczyk, H. R. Karimi, Shaping of the frequency response of vibrating plates with openings for vibro-acoustic systems, Mechanical Systems and Signal Processing 218 (2024) 111539. https://doi.org/10.1016/j.ymssp.2024.111539.

[7] B. Luk'Yanchuk, N. I. Zheludev, S. A. Maier, N. J. Halas, P. Nordlander, H. Giessen, C. T. Chong, The fano resonance in plasmonic nanostructures and metamaterials, Nature materials 9 (9) (2010) 707–715. https://doi.org/10.1038/nmat2810.

[8] L. Brillouin, Wave propagation in periodic structures (1946). https://doi.org/10.1038/158926a0.

[9] R. Martínez-Sala, Sound attenuation by sculpture, nature 378 (1995) 241. https://doi.org/10.1038/378241a0.

[10] F. J. Plantema, Sandwich construction: the bending and buckling of sandwich beams, plates, and shells (1966).
URL https://cir.nii.ac.jp/crid/1130282269423904128

[11] A. London, Transmission of reverberant sound through double walls, The journal of the acoustical society of America 22 (2) (1950) 270–279. https://doi.org/10.1121/1.1906601.

[12] C. B. Norris, An analysis of the compressive strength of honeycomb cores for sandwich construction, Tech. rep., NACA-TN-1251 (1947).
URL https://ntrs.nasa.gov/api/citations/19930082047/downloads/19930082047.pdf

[13] L. Wirt, Sound- absorptive materials to meet special requirements, The Journal of the Acoustical Society of America 57 (1) (1975) 126–143. https://doi.org/10.1121/1.380423.

[14] W. Tang, H. Zheng, C. Ng, Low frequency sound transmission through close-fitting finite sandwich panels, Applied Acoustics 55 (1) (1998) 13–30. https://doi.org/10.1016/S0003-682X(97)00107-2.

[15] S. Wang, X. Zhang, F. Li, S. M. Hosseini, Sound transmission loss of a novel acoustic metamaterial sandwich panel: Theory and experiment, Applied Acoustics 199 (2022) 109035. https://doi.org/10.1016/j.apacoust.2022.109035.

[16] X. Zhao, Z. Shuai, Y. Zhang, Z. Liu, Research on design method of metamaterial sound field control barrier based on transformer vibration and noise, Energy Reports 8 (2022) 1080–1089. https://doi.org/10.1016/j.egyr.2022.08.154.

[17] V. Cool, O. Sigmund, N. Aage, F. Naets, E. Deckers, Vibroacoustic topology optimization for sound transmission minimization through sandwich structures, Journal of Sound and Vibration 568 (2024) 117959. https://doi.org/10.1016/j.jsv.2023.117959.

[18] N. V. George, G. Panda, Advances in active noise control: A survey, with emphasis on recent nonlinear techniques, Signal processing 93 (2) (2013) 363–377. https://doi.org/10.1016/j.sigpro.2012.08.013.

[19] P. Lueg, Process of silencing sound oscillations, uS Patent 2043416 (June 9 1936).
URL https://cir.nii.ac.jp/crid/1574231874049765248

[20] J. C. Burgess, Active adaptive sound control in a duct: A computer simulation, The Journal of the Acoustical Society of America 70 (3) (1981) 715–726. https://doi.org/10.1121/1.386908.

[21] D. Morgan, An analysis of multiple correlation cancellation loops with a filter in the auxiliary path, IEEE Transactions on Acoustics, Speech, and Signal Processing 28 (4) (1980) 454–467. https://doi.org/10.1109/TASSP.1980.1163430.

[22] S. D. Stearns, Of aldapfive signal processing, Prentice-Hall, Inc., 1985.

[23] S.-C. Chan, Y. Chu, Performance analysis and design of fxlms algorithm in broadband anc system with online secondary-path modeling, IEEE transactions on audio, speech, and language processing 20 (3) (2011) 982–993. https://doi.org/10.1109/TASL.2011.2169789.

[24] P. Song, H. Zhao, Filtered-x least mean square/fourth (fxlms/f) algorithm for active noise control, Mechanical Systems and Signal Processing 120 (2019) 69–82. https://doi.org/10.1016/j.ymssp.2018.10.009.

[25] M. Ferrer, V. M. García-Mollá, A. M. Vidal-Maciá, M. de Diego, A. Gonzalez, Assessment of stability of distributed fxlms active noise control systems, Signal Processing 210 (2023) 109087. https://doi.org/10.1016/j.sigpro.2023.109087.

[26] Y. Pu, H. Zhou, Z. Meng, Multi-channel adaptive active vibration control of piezoelectric smart plate with online secondary path modelling using pzt patches, Mechanical Systems and Signal Processing 120 (2019) 166–179. https://doi.org/10.1016/j.ymssp.2018.10.019.

[27] H. Zheng, D. Yang, Z. Zhang, Active vibration control of time-varying structural systems with a logic fxlms algorithm, Journal of Aerospace Engineering 33 (4) (2020) 04020024. https://doi.org/10.1061/(ASCE)AS.1943-5525.0001131.

[28] S. Elliott, C. Boucher, Interaction between multiple feedforward active control systems, IEEE Transactions on Speech and Audio Processing 2 (4) (1994) 521–530. 10.1109/89.326611.

[29] M. Ferrer, M. de Diego, G. Piñero, A. Gonzalez, Active noise control over adaptive distributed networks, Signal Processing 107 (2015) 82–95. https://doi.org/10.1016/j.sigpro.2014.07.026.

[30] C. Antoñanzas, M. Ferrer, M. de Diego, A. Gonzalez, Collaborative method based on the acoustical interaction effects on active noise control systems over distributed networks, in: 2017 IEEE International Conference on Acoustics, Speech and Signal Processing (ICASSP), 2017, pp. 606–610. 10.1109/ICASSP.2017.7952227.

[31] T. Li, S. Lian, S. Zhao, J. Lu, I. S. Burnett, Distributed active noise control based on an augmented diffusion fxlms algorithm, IEEE/ACM Transactions on Audio, Speech, and Language Processing 31 (2023) 1449–1463. 10.1109/TASLP.2023.3261742.

[32] D. Moreau, B. Cazzolato, A. Zander, C. Petersen, A review of virtual sensing algorithms for active noise control, Algorithms 1 (2) (2008) 69–99. 10.3390/a1020069.

[33] C. Shi, Z. Jia, R. Xie, H. Li, An active noise control casing using the multi-channel feedforward control system and the relative path based virtual sensing method, Mechanical Systems and Signal Processing 144 (2020) 106878. 10.1016/j.ymssp.2020.106878.

[34] W. Jung, S. J. Elliott, J. Cheer, Estimation of the pressure at a listener's ears in an active headrest system using the remote microphone technique, The Journal of the Acoustical Society of America 143 (5) (2018) 2858–2869. 10.1121/1.5037363.

[35] M. Pawelczyk, Adaptive noise control algorithms for active headrest system, Control Engineering Practice 12 (9) (2004) 1101–1112. 10.1016/j.conengprac.2003.11.006.

[36] Z. Luo, D. Shi, W.-S. Gan, A hybrid sfanc-fxnlms algorithm for active noise control based on deep learning, IEEE Signal Processing Letters 29 (2022) 1102–1106. https://doi.org/10.1109/LSP.2022.3169428.

[37] D. Chen, L. Cheng, D. Yao, J. Li, Y. Yan, A secondary path-decoupled active noise control algorithm based on deep learning, IEEE Signal Processing Letters 29 (2021) 234–238. https://doi.org/10.1109/LSP.2021.3130023.

[38] Y.-J. Cha, A. Mostafavi, S. S. Benipal, Dnoisenet: Deep learning-based feedback active noise control in various noisy environments, Engineering Applications of Artificial Intelligence 121 (2023) 105971. https://doi.org/10.1016/j.engappai.2023.105971.

[39] M. Misol, S. Algermissen, M. Rose, H. P. Monner, Aircraft lining panels with low-cost hardware for active noise reduction, in: 2018 Joint Conference-Acoustics, IEEE, 2018, pp. 1–6. 10.1109/ACOUSTICS.2018.8502310.

[40] J. Milton, J. Cheer, S. Daley, Active structural acoustic control using an experimentally identified radiation resistance matrix, The Journal of the Acoustical Society of America 147 (3) (2020) 1459–1468. https://doi.org/10.1121/10.0000858.

[41] K. Mazur, S. Wrona, M. Pawelczyk, Design and implementation of multichannel global active structural acoustic control for a device casing, Mechanical Systems and Signal Processing 98 (2018) 877–889. https://doi.org/10.1016/j.ymssp.2017.05.025.

[42] C. Fuller, M. McLoughlin, S. Hildebrand, Active acoustic transmission loss box (April 28 1994).
URL https://patents.google.com/patent/US5692053A

[43] M. Pawelczyk, S. Wrona, Noise-Controlling Casings, CRC Press, 2022.
URL https://books.google.pl/books?id=NKN1EAAAQBAJ

[44] K. Mazur, M. Pawelczyk, Active control of noise emitted from a device casing, in: Proceedings of the 22nd International Congress of Sound and Vibration, Florence, Italy, 2015, pp. 12–16.

[45] K. Mazur, M. Pawelczyk, Internal model control for a light-weight active noise-reducing casing, Archives of Acoustics 41 (2) (2016).
URL https://acoustics.ippt.pan.pl/index.php/aa/article/view/1737

[46] K. Mazur, M. Pawelczyk, Virtual microphone control for a light-weight active noise-reducing casing, in: Proceedings of 23th International Congress on Sound and Vibration, Vol. 24, 2016, p. 411284. https://doi.org/10.4028/www.scientific.net/SSP.248.57.

[47] K. Mazur, S. Wrona, M. Pawelczyk, Active noise control for a washing machine, Applied Acoustics 146 (2019) 89–95. https://doi.org/10.1016/j.apacoust.2018.11.010.

[48] S. Masri, R. Miller, T. Dehghanyar, T. Caughey, Active parameter control of nonlinear vibrating structures, Journal of Applied Mechanics (1989). 10.1115/1.3176143.

[49] S. Wrona, M. Pawelczyk, L. Cheng, A novel semi-active actuator with tunable mass moment of inertia for noise control applications, Journal of Sound and Vibration 509 (2021) 116244. https://doi.org/10.1016/j.jsv.2021.116244.

[50] S. Wrona, M. Pawelczyk, L. Cheng, Sound transmission through a panel with a hybrid active and semi-active control system, Journal of Sound and Vibration 536 (2022) 117172. https://doi.org/10.1016/j.jsv.2022.117172.

[51] J. Jiang, Y. Li, Review of active noise control techniques with emphasis on sound quality enhancement, Applied Acoustics 136 (2018) 139–148. https://doi.org/10.1016/j.apacoust.2018.02.021.

[52] L. Lu, K.-L. Yin, R. C. de Lamare, Z. Zheng, Y. Yu, X. Yang, B. Chen, A survey on active noise control in the past decade–part ii: Nonlinear systems, Signal Processing 181 (2021) 107929. https://doi.org/10.1016/j.sigpro.2020.107929.

[53] Y. Guo, D. Shi, X. Shen, J. Ji, W.-S. Gan, A survey on adaptive active noise control algorithms overcoming the output saturation effect, Signal Processing (2024) 109525https://doi.org/10.1016/j.sigpro.2024.109525.

[54] F. Zangeneh-Nejad, R. Fleury, Active times for acoustic metamaterials, Reviews in Physics 4 (2019) 100031. https://doi.org/10.1016/j.revip.2019.100031.

[55] N. Gao, Z. Zhang, J. Deng, X. Guo, B. Cheng, H. Hou, Acoustic metamaterials for noise reduction: a review, Advanced Materials Technologies 7 (6) (2022) 2100698. https://doi.org/10.1002/admt.202100698.

[56] Y. Tao, M. Ren, H. Zhang, T. Peijs, Recent progress in acoustic materials and noise control strategies–a review, Applied Materials Today 24 (2021) 101141. https://doi.org/10.1016/j.apmt.2021.101141.

[57] R. Yurkovich, J. Schmidt, A. Zak, Dynamic analysis of stiffened panel structures, Journal of Aircraft 8 (3) (1971) 149–155. https://doi.org/10.2514/3.44246.

[58] M. Olson, C. Hazell, Vibration studies on some integral rib-stiffened plates, Journal of Sound and Vibration 50 (1) (1977) 43–61. https://doi.org/10.1016/0022-460X(77)90550-8.

[59] M. Amabili, M. Pellegrini, F. Righi, F. Vinci, Effect of concentrated masses with rotary inertia on vibrations of rectangular plates, Journal of sound and vibration 295 (1-2) (2006) 1–12. https://doi.org/10.1016/j.jsv.2005.11.035.

[60] S. Le Moyne, J.-L. Tebec, I. Tawfiq, Acoustical influence of stiffeners on acoustic radiation of plates, Mechanical systems and signal processing 19 (1) (2005) 195–212. https://doi.org/10.1016/S0888-3270(03)00054-2.

[61] J. P. Arenas, Matrix method for estimating the sound power radiated from a vibrating plate for noise control engineering applications, Latin American applied research 39 (4) (2009) 345–352.

[62] M. Barrette, A. Berry, O. Beslin, Vibration of stiffened plates using hierarchical trigonometric functions, Journal of Sound and Vibration 235 (5) (2000) 727–747. https://doi.org/10.1006/jsvi.2000.2978.

[63] S. Wrona, M. Pawelczyk, Shaping frequency response of a vibrating plate for passive and active control applications by simultaneous optimization of arrangement of additional masses and ribs. part i: Modeling, Mechanical Systems and Signal Processing 70 (2016) 682–698. https://doi.org/10.1016/j.ymssp.2015.08.018.

[64] S. Shi, T. Guo, B. Xiao, G. Jin, C. Gao, Modelling and analysis of vibro-acoustic coupled spaces with a mixed interface, Mechanical Systems and Signal Processing 158 (2021) 107788. https://doi.org/10.1016/j.ymssp.2021.107788.

[65] Z. Zhu, Y. Song, Y. Zhang, Q. Liu, G. Wang, Sound radiation of the plate with arbitrary holes, International Journal of Mechanical Sciences 264 (2024) 108814. https://doi.org/10.1016/j.ijmecsci.2023.108814.

[66] J. Mei, G. Ma, M. Yang, Z. Yang, W. Wen, P. Sheng, Dark acoustic metamaterials as super absorbers for low-frequency sound, Nature communications 3 (1) (2012) 756. https://doi.org/10.1038/ncomms1758.

[67] Y. Duan, J. Luo, G. Wang, Z. H. Hang, B. Hou, J. Li, P. Sheng, Y. Lai, Theoretical requirements for broadband perfect absorption of acoustic waves by ultra-thin elastic meta-films, Scientific Reports 5 (1) (2015) 12139. https://doi.org/10.1038/srep12139.

[68] J. Christensen, V. Romero-García, R. Picó, A. Cebrecos, F. G. De Abajo, N. A. Mortensen, M. Willatzen, V. J. Sánchez-Morcillo, Extraordinary absorption of sound in porous lamella-crystals, Scientific reports 4 (1) (2014) 4674. https://doi.org/10.1038/srep04674.

[69] L. Fan, Z. Chen, S.-y. Zhang, J. Ding, X.-j. Li, H. Zhang, An acoustic metamaterial composed of multi-layer membrane-coated perforated plates for low-frequency sound insulation, Applied Physics Letters 106 (15) (2015). https://doi.org/10.1063/1.4918374.

[70] N. Sui, X. Yan, T.-Y. Huang, J. Xu, F.-G. Yuan, Y. Jing, A lightweight yet sound-proof honeycomb acoustic metamaterial, Applied Physics Letters 106 (17) (2015). https://doi.org/10.1063/1.4919235.

[71] S. Elliott, Signal processing for active control, Elsevier, 2000. https://doi.org/10.1016/B978-0-12-237085-4.X5000-5.

[72] R. Harris, D. Chabries, F. Bishop, A variable step (vs) adaptive filter algorithm, IEEE transactions on acoustics, speech, and signal processing 34 (2) (1986) 309–316. https://doi.org/10.1109/TASSP.1986.1164814.

[73] S. M. Kuo, D. R. Morgan, Active noise control systems, Vol. 4, Wiley, New York, 1996.
URL https://www.academia.edu/download/49705683/DE0048E46640B42D4E294C12576430058275B.pdf

[74] M. Bouchard, S. Quednau, Multichannel recursive-least-square algorithms and fast-transversal-filter algorithms for active noise control and sound reproduction systems, IEEE transactions on speech and audio processing 8 (5) (2000) 606–618. https://doi.org/10.1109/89.861382.

[75] F. Albu, M. Bouchard, Y. Zakharov, Pseudo-affine projection algorithms for multichannel active noise control, IEEE transactions on audio, speech, and language processing 15 (3) (2007) 1044–1052. https://doi.org/10.1109/TASL.2006.881677.

[76] Á. A. Vázquez, E. Pichardo, J. G. Avalos, G. Sánchez, H. M. Martínez, J. C. Sánchez, H. M. Pérez, Multichannel active noise control based on filtered-x affine projection-like and lms algorithms with switching filter selection, Applied Sciences 9 (21) (2019) 4669. https://doi.org/10.3390/app9214669.

[77] M. De Diego, A. Gonzalez, M. Ferrer, G. Pinero, An adaptive algorithms comparison for real multi-channel active noise control, in: 2004 12th European Signal Processing Conference, IEEE, 2004, pp. 925–928.

[78] S. Elliott, I. Stothers, P. Nelson, A multiple error lms algorithm and its application to the active control of sound and vibration, IEEE Transactions on Acoustics, Speech, and Signal Processing 35 (10) (1987) 1423–1434. 10.1109/TASSP.1987.1165044.

[79] S. C. Douglas, Fast implementations of the filtered-x lms and lms algorithms for multichannel active noise control, IEEE Transactions on speech and audio processing 7 (4) (1999) 454–465. https://doi.org/10.1109/89.771315.

[80] E. Esmailzadeh, A. Ohadi, A. Alasty, Multi-channel adaptive feedforward control of noise in an acoustic duct, J. Dyn. Sys., Meas., Control 126 (2) (2004) 406–415. https://doi.org/10.1115/1.1636772.

[81] B. Mazeaud, M.-A. Galland, A multi-channel feedback algorithm for the development of active liners to reduce noise in flow duct applications, Mechanical Systems and Signal Processing 21 (7) (2007) 2880–2899. https://doi.org/10.1016/j.ymssp.2007.02.009.

[82] N. Devineni, I. Panahi, P. Kasbekar, Predictive multi-channel feedback active noise control for hvac systems, in: 2011 IEEE INTERNATIONAL CONFERENCE ON ELECTRO/INFORMATION TECHNOLOGY, IEEE, 2011, pp. 1–5. https://doi.org/10.1109/EIT.2011.5978581.

[83] N. Botti, T. Botti, L. Liu, R. Corradi, F. Ripamonti, Active structural-acoustic control on interior noise of a plate-cavity system using fxnlms algorithm, Available at SSRN 4794801 (2021). https://dx.doi.org/10.2139/ssrn.4794801.

[84] A. Chraponska, S. Wrona, J. Rzepecki, K. Mazur, M. Pawelczyk, Active structural acoustic control of an active casing placed in a corner, Applied Sciences 9 (6) (2019). 10.3390/app9061059.
URL https://www.mdpi.com/2076-3417/9/6/1059

[85] Y. Xiao, L. Ma, K. Hasegawa, Properties of fxlms-based narrowband active noise control with online secondary-path modeling, IEEE Transactions on Signal Processing 57 (8) (2009) 2931–2949. https://doi.org/10.1109/TSP.2009.2020766.

[86] M. Zhang, H. Lan, W. Ser, Cross-updated active noise control system with online secondary path modeling, IEEE Transactions on speech and audio processing 9 (5) (2001) 598–602. https://doi.org/10.1109/89.928924.

[87] A. Krishna, L. Ravinchandra, T. K. Fei, L. C. Yong, Active noise reduction using lms and fxlms algorithms, in: Journal of Physics: Conference Series, Vol. 1228, IOP Publishing, 2019, p. 012064. 10.1088/1742-6596/1228/1/012064.

[88] W. Li, W. Wang, B. Li, Z. Yang, Error signal differential term feedback enhanced variable step size fxlms algorithm for piezoelectric active vibration control, Shock and Vibration 2020 (1) (2020) 8832467. https://doi.org/10.1155/2020/8832467.

[89] C. Antoñanzas, M. Ferrer, A. Gonzalez, M. de Diego, G. Pinero, Diffusion algorithm for active noise control in distributed networks, in: Proceedings of the 22nd International Congress on Sound and Vibration, 2015.

[90] C. Antoñanzas, M. Ferrer, M. de Diego, A. Gonzalez, Remote microphone technique for active noise control over distributed networks, IEEE/ACM Transactions on Audio, Speech, and Language Processing 31 (2023) 1522–1535. 10.1109/TASLP.2023.3264600.

[91] C. Antoñanzas, M. Ferrer, M. de Diego, A. Gonzalez, Affine-projection-like algorithm for active noise control over distributed networks, in: 2016 IEEE Sensor Array and Multichannel Signal Processing Workshop (SAM), 2016, pp. 1–5. 10.1109/SAM.2016.7569696.

[92] C. Antoñanzas, M. Ferrer, M. de Diego, A. Gonzalez, Control effort strategies for acoustically coupled distributed acoustic nodes, Wireless Communications and Mobile Computing 2017 (1) (2017) 3601802. https://doi.org/10.1155/2017/3601802.

[93] Y. Chu, C. Mak, Y. Zhao, S. Chan, M. Wu, Performance analysis of a diffusion control method for anc systems and the network design, Journal of Sound and Vibration 475 (2020) 115273. https://doi.org/10.1016/j.jsv.2020.115273.

[94] Y. Dong, J. Chen, W. Zhang, Wave-domain active noise control over distributed networks of multichannel nodes, Signal Processing 184 (2021) 108050. https://doi.org/10.1016/j.sigpro.2021.108050.

[95] J. Ji, D. Shi, Z. Luo, X. Shen, W.-S. Gan, A practical distributed active noise control algorithm overcoming communication restrictions, in: ICASSP 2023 - 2023 IEEE International Conference on Acoustics, Speech and Signal Processing (ICASSP), 2023, pp. 1–5. 10.1109/ICASSP49357.2023.10097013.

[96] C. K. Lai, J. S. Tey, D. Shi, W.-S. Gan, Robust estimation of open aperture active control systems using virtual sensing, in: INTER-NOISE and NOISE-CON Congress and Conference Proceedings, Vol. 265, Institute of Noise Control Engineering, 2023, pp. 3397–3407.

[97] S. J. Elliott, J. Zhang, C. K. Lai, J. Cheer, Superposition of the uncertainties in acoustic responses and the robust design of active control systems, The Journal of the Acoustical Society of America 148 (3) (2020) 1415–1424. 10.1121/10.0001965.

[98] Z. Zhang, M. Wu, L. Yin, C. Gong, J. Yang, Y. Cao, L. Yang, Robust parallel virtual sensing method for feedback active noise control in a headrest, Mechanical Systems and Signal Processing 178 (2022) 109293. 10.1016/j.ymssp.2022.109293.

[99] J. Zhang, S. J. Elliott, J. Cheer, Robust performance of virtual sensing methods for active noise control, Mechanical Systems and Signal Processing 152 (2021) 107453. 10.1016/j.ymssp.2020.107453.

[100] C. Shi, R. Xie, N. Jiang, H. Li, Y. Kajikawa, Selective Virtual Sensing Technique for Multi-channel Feedforward Active Noise Control Systems, in: ICASSP 2019 - 2019 IEEE International Conference on Acoustics, Speech and Signal Processing (ICASSP), IEEE, Brighton, United Kingdom, 2019, pp. 8489–8493. 10.1109/ICASSP.2019.8682705.

[101] R. Xie, A. Tu, C. Shi, S. Elliott, H. Li, L. Zhang, Cognitive Virtual Sensing Technique for Feedforward Active Noise Control, in: ICASSP 2024 - 2024 IEEE International Conference on Acoustics, Speech and Signal Processing (ICASSP), IEEE, Seoul, Korea, Republic of, 2024, pp. 981–985. 10.1109/ICASSP48485.2024.10446463.

[102] D. Shi, W.-S. Gan, B. Lam, R. Hasegawa, Y. Kajikawa, Feedforward multichannel virtual-sensing active control of noise through an aperture: Analysis on causality and sensor-actuator constraints, The Journal of the Acoustical Society of America 147 (1) (2020) 32–48. 10.1121/10.0000515.

[103] H. Zhang, D. Wang, Deep anc: A deep learning approach to active noise control, Neural Networks 141 (2021) 1–10. https://doi.org/10.1016/j.neunet.2021.03.037.

[104] Z.-Q. Wang, P. Wang, D. Wang, Multi-microphone complex spectral mapping for utterance-wise and continuous speech separation, IEEE/ACM transactions on audio, speech, and language processing 29 (2021) 2001–2014. https://doi.org/10.1109/TASLP.2021.3083405.

[105] Z.-Q. Wang, P. Wang, D. Wang, Complex spectral mapping for single- and multi-channel speech enhancement and robust asr, IEEE/ACM Transactions on Audio, Speech, and Language Processing 28 (2020) 1778–1787. 10.1109/TASLP.2020.2998279.

[106] Y. Yao, T.-S. Chang, Asc: Adaptive scale feature map compression for deep neural network, IEEE Transactions on Circuits and Systems I: Regular Papers (2023). https://doi.org/10.1109/TCSI.2023.3337283.

[107] D. Wu, X. Wu, T. Qu, A hybrid deep-online learning based method for active noise control in wave domain, in: ICASSP 2024-2024 IEEE International Conference on Acoustics, Speech and Signal Processing (ICASSP), IEEE, 2024, pp. 1301–1305. https://doi.org/10.1109/ICASSP48485.2024.10446791.

[108] H. Zhang, A. Pandey, D. Wang, Attentive recurrent network for low-latency active noise control., in: INTERSPEECH, 2022, pp. 956–960.

[109] Y. A. Zhang, F. Ma, T. D. Abhayapala, P. N. Samarasinghe, A. Bastine, An active noise control system based on soundfield interpolation using a physics-informed neural network, in: ICASSP 2024-2024 IEEE International Conference on Acoustics, Speech and Signal Processing (ICASSP), IEEE, 2024, pp. 506–510. https://doi.org/10.1109/ICASSP48485.2024.10447208.

[110] Y. Kajikawa, W.-S. Gan, S. M. Kuo, Recent advances on active noise control: open issues and innovative applications, APSIPA Transactions on Signal and Information Processing 1 (2012) e3. 10.1115/1.4011984.

[111] B. Hassibi, A. Sayed, T. Kailath, H infinity optimality of the lms algorithm, IEEE Transactions on Signal Processing 44 (2) (1996) 267–280. 10.1109/78.485923.

[112] K. Mazur, S. Wrona, A. Chraponska, J. Rzepecki, M. Pawelczyk, Fxlms with multiple error switching for active noise-cancelling casings., Archives of Acoustics 44 (4) (2019) 775 – 782. http://dx.doi.org/10.24425/aoa.2019.129732.

[113] D. Bismor, Simulations of partial update lms algorithms in application to active noise control, Procedia Computer Science 80 (2016) 1180–1190. https://doi.org/10.1016/j.procs.2016.05.451.

[114] M. Godavarti, A. O. Hero, Partial update lms algorithms, IEEE Transactions on signal processing 53 (7) (2005) 2382–2399. https://doi.org/10.1109/TSP.2005.849167.

[115] W. Wang, J. Li, M. Li, Selective partial update of nlms adaptive filter algorithm, in: Journal of Physics: Conference Series, Vol. 1966, IOP Publishing, 2021, p. 012009. 10.1088/1742-6596/1966/1/012009.

[116] Z. Qing, J. Ni, Z. Li, J. Chen, Selective partial-update augmented complex-valued lms algorithm and its performance analysis, Signal Processing 188 (2021) 108217. https://doi.org/10.1016/j.sigpro.2021.108217.

[117] D. Bismor, Leaky partial update lms algorithms in application to structural active noise control, Sensors 23 (3) (2023). 10.3390/s23031169.
URL https://www.mdpi.com/1424-8220/23/3/1169

[118] D. Bismor, Leaky partial updates to control a real device casing, Vibrations in Physical Systems 33 (3) (2022). http://dx.doi.org/10.21008/j.0860-6897.2022.3.04.

[119] B. Widrow, Adaptive filters, Aspects of network and system theory (1971).
URL https://isl.stanford.edu/~widrow/papers/b1971adaptivefilters.pdf

[120] S. C. Douglas, A family of normalized lms algorithms, IEEE signal processing letters 1 (3) (1994) 49–51. https://doi.org/10.1109/97.295321.

[121] S. Douglas, Analysis and implementation of the max-nlms adaptive filter, in: Conference Record of The Twenty-Ninth Asilomar Conference on Signals, Systems and Computers, Vol. 1, IEEE, 1995, pp. 659–663. https://doi.org/10.1109/ACSSC.1995.540631.

[122] S. Haykin, Adaptive Filter Theory, Prentice-Hall information and system sciences series, Prentice Hall, 1996.
URL https://books.google.pl/books?id=178QAQAAMAAJ

[123] T. Aboulnasr, K. Mayyas, Mse analysis of the m-max nlms adaptive algorithm, in: Proceedings of the 1998 IEEE International Conference on Acoustics, Speech and Signal Processing, ICASSP'98 (Cat. No. 98CH36181), Vol. 3, IEEE, 1998, pp. 1669–1672. https://doi.org/10.1109/ICASSP.1998.681776.

[124] K. Mayyas, T. Aboulnasr, T. Eldos, A study of the robustness of the m-max nlms adaptive algorithm, in: 1999 IEEE International Symposium on Circuits and Systems (ISCAS), Vol. 3, IEEE, 1999, pp. 154–157. https://doi.org/10.1109/ISCAS.1999.778808.

[125] K. Mayyas, T. Aboulnasr, Leaky lms algorithm: Mse analysis for gaussian data, IEEE Transactions on Signal Processing 45 (4) (1997) 927–934. https://doi.org/10.1109/78.564181.

[126] T. Aboulnasr, K. Mayyas, Selective coefficient update of gradient-based adaptive algorithms, in: 1997 IEEE International Conference on Acoustics, Speech, and Signal Processing, Vol. 3, IEEE, 1997, pp. 1929–1932. https://doi.org/10.1109/ICASSP.1997.598919.

[127] S. C. Douglas, Adaptive filters employing partial updates, IEEE Transactions on Circuits and Systems II: Analog and Digital Signal Processing 44 (3) (1997) 209–216. https://doi.org/10.1109/82.558455.

[128] M. Godavarti, A. Hero, Stability analysis of the sequential partial update lms algorithm, in: 2001 IEEE International Conference on Acoustics, Speech, and Signal Processing. Proceedings (Cat. No. 01CH37221), Vol. 6, IEEE, 2001, pp. 3857–3860. https://doi.org/10.1109/ICASSP.2001.940685.

[129] K. Mazur, S. Wrona, M. Pawelczyk, Placement of microphones for an active noise-reducing casing, in: Proceedings of the 25th International Congress on Sound and Vibration, Hiroshima, Japan, 2018, pp. 8–12.